Force and phosphate release from Arp2/3 complex promote dissociation of actin filament branches

Authors: Nandan G. Pandit[a,d], Wenxiang Cao[a], Jeffrey Bibeau[a], Eric M. Johnson-Chavarria[a], Edwin W. Taylor[a], Thomas D. Pollard[a,b,c,d], Enrique M. De La Cruz[a,1]

[a] Department of Molecular Biophysics and Biochemistry, Yale University, New Haven, CT 06520
[b] Department of Molecular, Cellular, and Developmental Biology, Yale University, New Haven, CT 06520
[c] Department of Cell Biology, Yale University, New Haven, CT 06520
[d] Program in Physical and Engineering Biology, Yale University, New Haven, CT 06520
[1] Corresponding author (email: enrique.delacruz@yale.edu phone number: +1 (203) 432-5424)

Supplemental Information Appendix

Part 1. Supplementary figures and movies

Part 2. Two-state model for actin network debranching

Part 3. A model for the distribution of branches at the leading edge of cells based on the dependence of the rates of branch dissociation on age and applied force.

Part 4. DNA sequence of GMF

www.pnas.org/cgi/doi/10.1073/pnas.1911183117

Part 1. Supplementary figures and movies

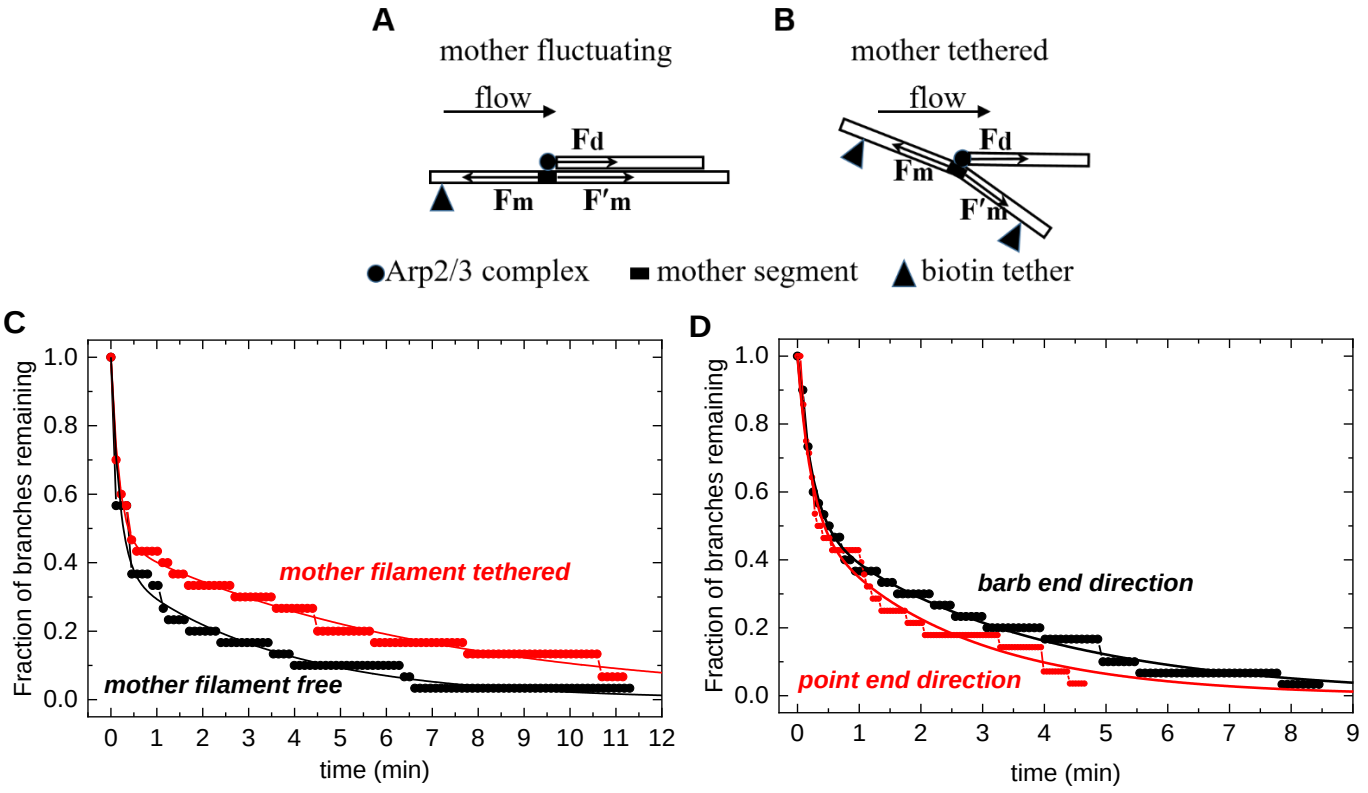

Fig. S1. Time courses of debranching depend weakly on tension in the mother filament and the direction of force. A and B. Free body diagram illustrating the forces acting on a mother filament segment (filled rectangular block) with a bound daughter filament. One force ($\mathbf{F_d}$) originates from pulling of the freely moving daughter filament. This force in the direction of flow scales with the daughter filament length and flow rate (Eq. 5). The other two forces originate from pulling of the flanking mother filament segments at each side ($\mathbf{F_m}$ and $\mathbf{F'_m}$) of the branch. For a freely fluctuating mother filament, $\mathbf{F_m}$ and $\mathbf{F'_m}$ align with the flow direction, but in opposite directions (A). When the entire mother filament is tethered, the orientations of $\mathbf{F_m}$ and $\mathbf{F'_m}$ are confined and do not align with flow. The amplitudes of $\mathbf{F_m}$ and $\mathbf{F'_m}$ vary with geometry (B). The tension induced in the mother filament segment with a branch must counter-balance all the three forces acting on it. C and D. Branched actin networks were assembled for ~4 min with the entire mother filament or just a pointed end segment tethered to the surface. Without additional aging, the time courses of debranching followed double exponentials (n = 30 branches) under 500 µL min^{-1} buffer flow (~1.02 pN of force for a branch of 1.5 µm). C. Time courses of branch dissociation from tethered and freely fluctuating mother filaments with the buffer flow at 500 µL min^{-1}. The smooth lines through data are the best double exponential fits, yielding fast phase lifetimes of 0.19 (±0.02; free) and 0.18 (±0.01; tethered) min, amplitudes of 18 vs. 16%, and slow phase lifetimes of 3.5 (±0.2; free) and 6.8 (±0.2; tethered) min. The uncertainties represent the standard deviations from the fits. The force on immobilized mother filaments depends on their (random) orientations, while freely-fluctuating mother filaments align with flow and experience tension in a single direction. Thirty branches were scored for both free and tethered mother filament conditions. D. Time courses of branch dissociation with the buffer flow at 500 µL min^{-1} towards the barbed or pointed ends of mother filaments oriented parallel to the direction of flow and tethered to the surface throughout their lengths. Flow toward the mother filament barbed end pushed branches "forward", while flow towards the mother filament pointed end pushed branches "backward". n =30 for the barbed end direction and n =28 for the pointed end. See Movie S6-7). The smooth lines through data are the best fits to double exponentials, yielding fast phase lifetimes of 0.23 (±0.02; barbed) and 0.22 (±0.02; pointed) min, amplitudes of 49 vs. 48%, and slow phase lifetimes of 3.5 (±0.1; barbed) and 2.4 (±0.1; pointed) min. The uncertainties represent the standard deviations from the fits.

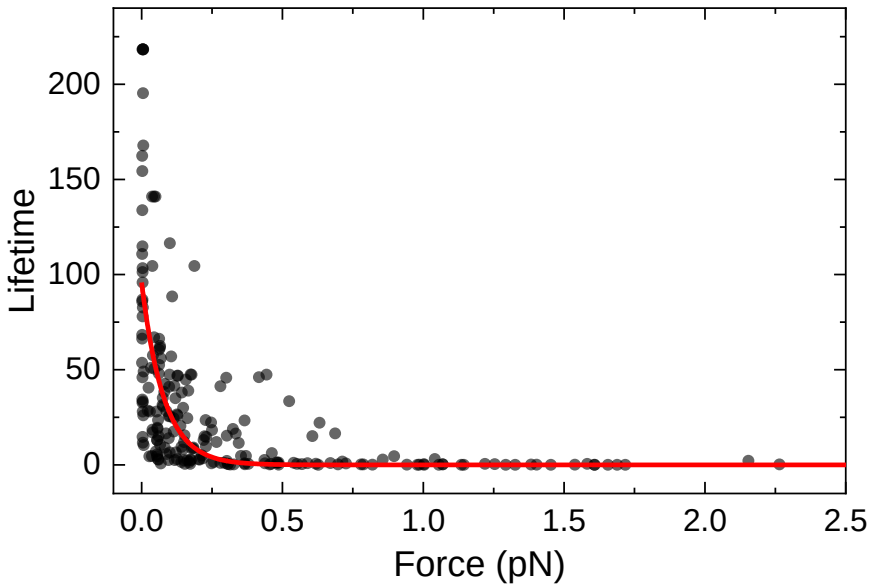

Fig. S2. (Previous Fig. 2D inset) Rug plot analysis of dependence of branch lifetimes on force for branches formed from ATP-Arp2/3 complex and aged for 30 min to form branches with ADP-Arp2/3 complex (time courses in Fig. 2A). Force dependence of individual branch lifetimes was fitted to Bell's equation (Eq. 1) for comparison. The best fit resulted in characteristic distance d = 52 (± 7) nm (F1/2 = 0.054 (± 0.008) pN) and branch lifetime with 0 force τ_0 = 96 (± 6) min (rate constant = τ_0^{-1} = 0.01 (± 0.007) min^{-1}).

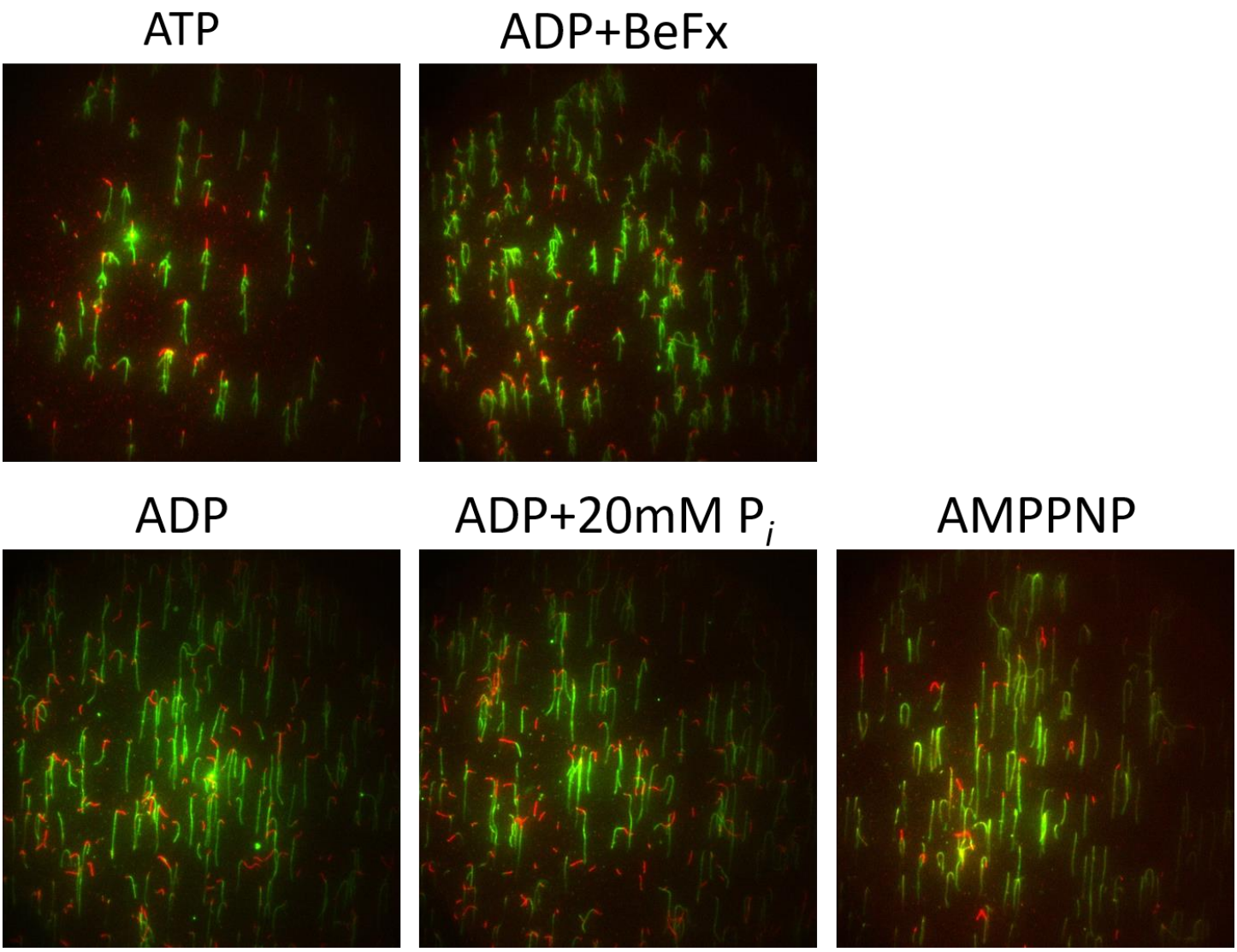

Fig. S3. Fluorescence micrographs of actin filaments in the presence of Arp2/3 complex in the flow chamber. Experimental set-up and fluorescent labeling are as described in Fig 1A. The flow rate is ≤25 μL min $^{-1}$. Upper row: ATP-actin and ATP-Arp2/3 complex (ATP) and ADP-actin ADP-BeF$_x$-Arp-2/3 complex (ADP+BeFx) prepared from ADP-Arp2/3 with 2 mM $BeSO_4$ + 10 mM NaF robustly form branches. Lower row: Neither ADP-actin and ADP-Arp2/3 complex, with or without 20 mM P_i (ADP, ADP+20 mM P_i), nor AMPPNP-actin and AMPPNP-Arp2/3 complex (AMPPNP) form branches under our experimental conditions.

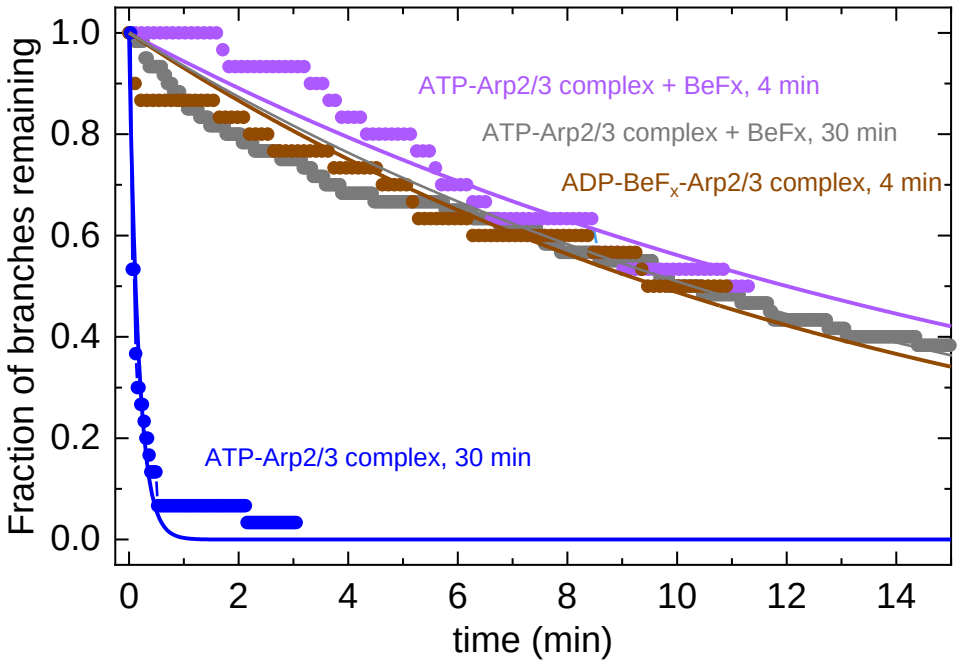

Fig. S4. Dissociation time courses of branches formed from ATP- or ADP-Arp2/3 complex in the presence or absence of BeF_x and aged for various times. Debranching was observed under force by applying 500 μL min^{-1} (approximately 1.02 pN for a branch of 1.5 μm). All time courses follow single exponentials with observed lifetimes of 0.21 (±0.02) min^{-1} for ATP-Arp2/3 complex aged for 30 min (blue), 13.9 (±0.2) min^{-1} for ADP-Arp2/3 complex in the presence of 2mM BeF_x and aged for ~4 min (brown), and 17.3 (±0.03) min^{-1} and 14.8 (±0.09) min^{-1} for branches formed with ATP-Arp2/3 complex in the presence of 2mM BeF_x and aged for ~4 min (purple) or 30 min (gray), respectively.

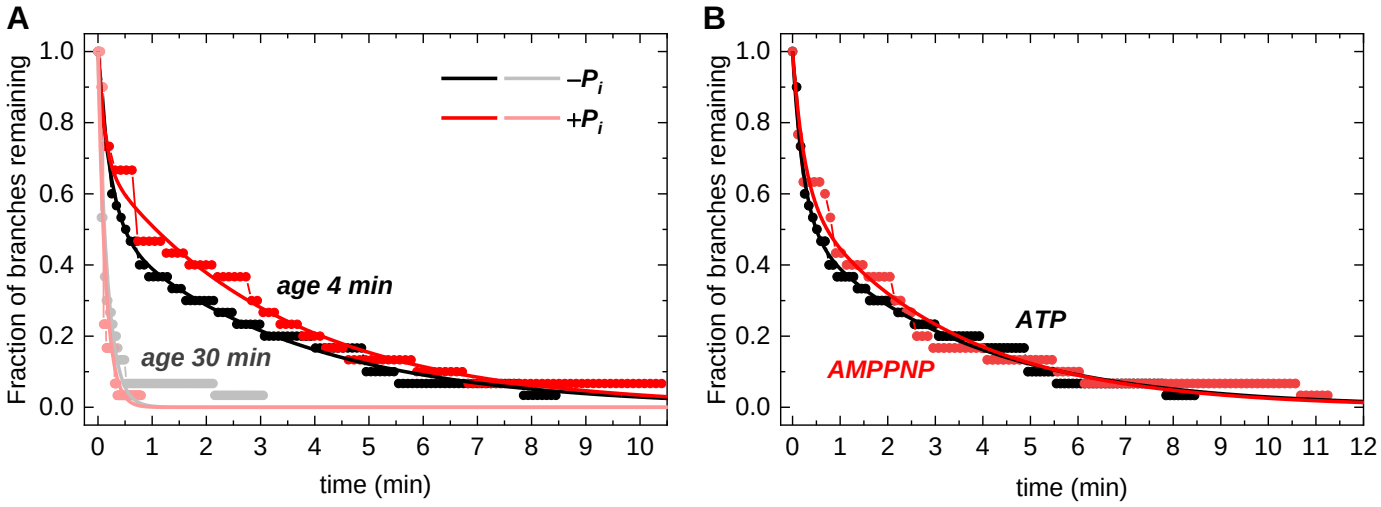

Fig. S5. The time course of debranching does not depend on the nucleotide state of the mother filament. (A) Comparison of the time courses of dissociation of branches assembled in polymerization buffer containing 0.2 mM ATP with 0 or 20 mM potassium phosphate and aged for ~4 min (dark colored traces) or 30 min (light colored traces) before observing the time course of branch dissociation at a buffer flow of 500 μL min^{-1} (approximately 1.02 pN of force for a branch of 1.5 μm). Phosphate (20 mM) saturates ADP-actin filaments to form ADP-P_i actin mother and daughter filaments. The affinity of ADP-Arp2 or Arp3 in branch junctions for phosphate is not known. *n* = 30 for all traces. The smooth lines through data are the best double exponential fits (~4 min aging, fast phase lifetime = 0.23 (±0.02; –P_i) and 0.12 (±0.02; +P_i) min, amplitude 0.47 vs. 0.3% and slow phase lifetime = 3.5 (±0.1; –P_i) and 3.3 (±0.1; +P_i) min) or single exponential (30 min aging; lifetime = 0.17 (±0.01; –P_i) and 0.14 (±0.01; +P_i) min). The uncertainties represent the standard deviations of the best fits of the data to single or double exponentials. (B) Comparison of the time courses of dissociation of branches assembled from ATP-Arp2/3 complex and ATP- or AMPPNP-actin monomers in polymerization buffer with 0.2 mM ATP or AMPPNP. After aging branches for ~4 min force was applied by buffer flowing at 500 μL min^{-1}. *n* = 30 branches for both conditions. The smooth lines through data are the best double exponential fits with slow phase lifetime of 3.5 (±0.1; ATP) vs. 3.2 (±0.1, AMPPNP) min and fast phase lifetime of 0.23 (±0.02; ATP) vs. 0.25 (±0.04, AMPPNP) min. The fast phase amplitude is 0.49 vs. 0.4%. The uncertainties represent the standard deviations of the best fits of the data to double exponentials.

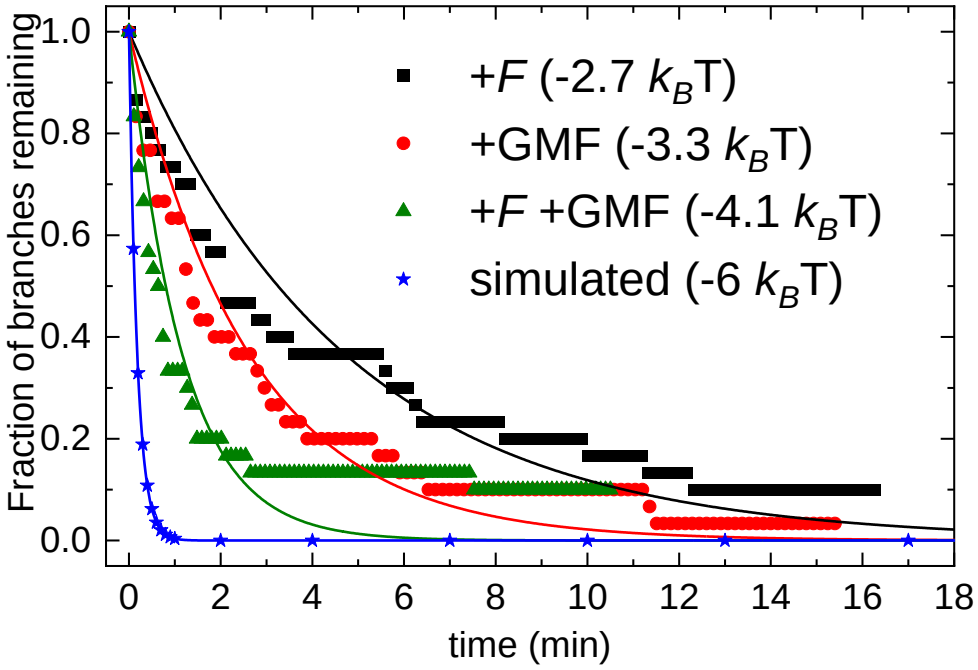

Fig. S6. Force and GMF together accelerate debranching of ADP-Arp2/3 complex branches more than either does alone. Branches were formed as described in *Methods* and aged for 30 min to form ADP-Arp2/3 complex branches. Debranching was then initiated with 15 (very weak force – approximately 0.03 pN for a 1.5 μm branch) or 125 μL min^{-1} (moderate force – approximately 0.25 pN for a 1.5 μm branch) flow with and without 500 nM GMF. Those time courses follow single exponential decays (Fig. 2A). Debranching of ADP-Arp2/3 complex branches under 125 μL min^{-1} flow was ~15-fold faster than under 15 μL min^{-1} flow (lifetime reduced from 71 to 4.7 min, filled black squares), corresponding to a reduction in debranching activation energy of 2.7 k_BT ($\Delta\Delta G^{\ddagger} = k_BT \ln(\tau_2/\tau_1)$. Inclusion of 500 nM GMF alone accelerated ADP-Arp2/3 complex branch debranching ~27 fold compared to that under weaker flow (15 μL min^{-1}) without GMF (lifetime from 71 to 2.6 min, filled red circles) and reduced the debranching activation energy by 3.3 k_BT. Force (125 μL min^{-1} flow) and GMF (500 nM) together further accelerate debranching of ADP-Arp2/3 complex branches, shortening the lifetime from 71 to 1.16 min (filled green triangles), corresponding to a reduction in debranching activation energy of 4.1 k_BT. This reduction in debranching activation energy less than the sum of 6 k_BT predicted if the effects of force and GMF were additive. A simulated debranching time course with an activation energy reduction of 6 k_BT with corresponding lifetime of 0.18 min is shown for comparison (filled blue stars). The uncertainties were propagated from standard deviation in the lifetime obtained from the best exponential fits.

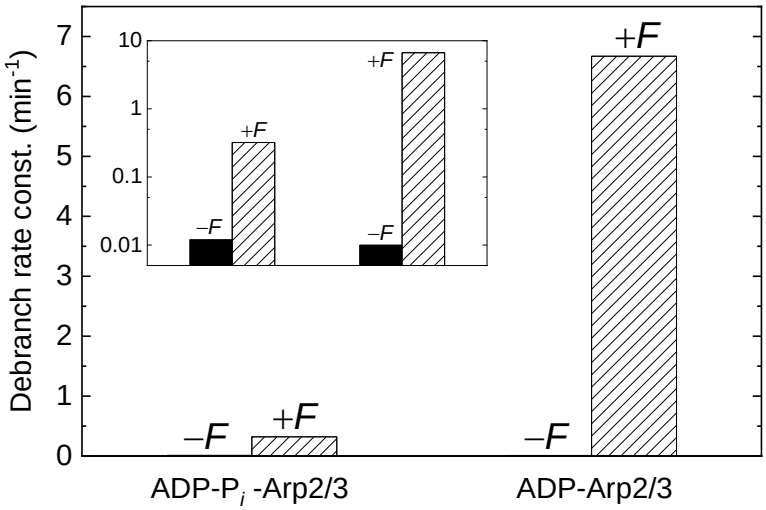

Fig. S7. Branches with ADP-Arp2/3 complex are far more sensitive to debranching by force than ADP-P$_i$-Arp2/3 complex. The debranching rate constants in the absence of force for ADP-P$_i$-Arp2/3 complex (k_1) and ADP-Arp2/3 branches (k_2) were determined from analysis of data in Figs. 2 and 4 (Table 1). The global double exponential fits of the aging time-dependence of debranching time courses (Fig. 2B) yielded the observed slow ($k_{s,F}$) and ($k_{f,F}$) phase rate constant under 500 μL min^{-1} flow force. The rate constant for ADP-Arp2/3 complex debranching under force ($k_{2,F}$) is the fast, observed rate constant (i.e. $k_{2,F} = k_{f,F}$), whereas the slow observed rate constant represents a composite of the rate constants for ADP-P$_i$-Arp2/3 complex debranching ($k_{1,F}$) and conversion ($k_{conv,F}$) under force (i.e. $k_{s,F} = k_{1,F} + k_{conv,F}$; Eq. S41). Accordingly, $k_{1,F}$ can be estimated as $k_1 \leq k_{1,F} < k_{s,F}$. The upper limit, where $k_{1,F} = k_{s,F}$, is plotted. The actual $k_{1,F}$ value under force is therefore smaller than plotted. Note that the y-axis of the inset is on a logarithmic scale.

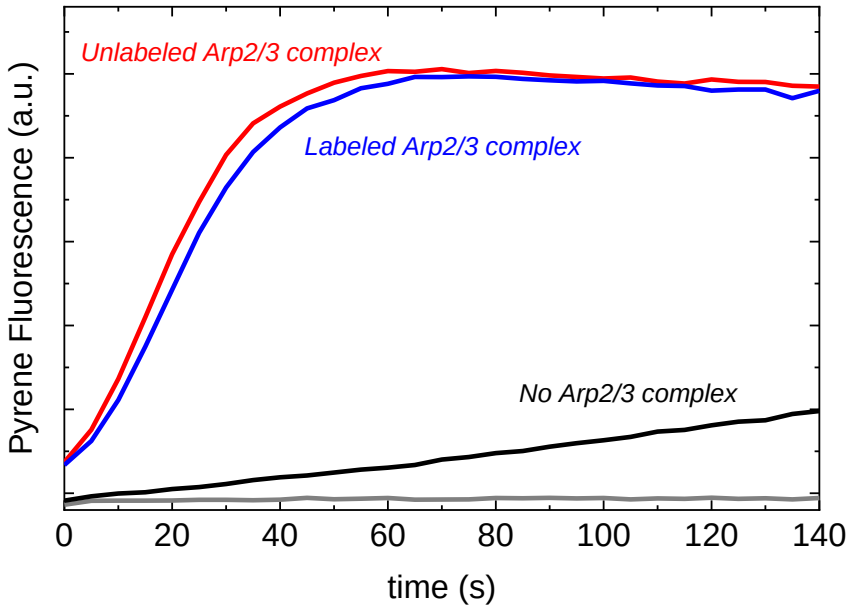

Fig S8. Comparison of the nucleation activity of Arp2/3 complex without a label and with Alexa-488 conjugated to a snap tag on the Arpc5 subunit monitored by the time course of pyrenyl-actin polymerization. Conditions: 3 µM actin monomers (30% pyrene labeled), 200 nM Arp2/3 complex (± 82% Alexa-488 labeled), and 500 nM GST-VCA at 25 °C. Reactants were mixed at time zero and fluorescence emission was recorded at 407 nm (excitation wavelength = 365 nm) in a plate reader (Molecular Devices, SpectraMax GEMINI XPS). Red curve: unlabeled Arp2/3 complex in KMIE polymerization buffer; Blue curve: Alexa-488 Snap ArpC5 Arp2/3 complex in KMIE polymerization buffer; Black curve: 30% labeled pyrene monomers alone (no Arp2/3 complex) in KMIE polymerization buffer; Grey curve: 30% labeled pyrene actin monomers alone in low salt, non-polymerizing, G-buffer (1).

Videos

Time lapse movies of fluorescence micrographs at different frame rates and flow rates showing dissociation of a branches formed by Arp2/3 complex. Filament seeds containing 15% 568-Alexa and 10% biotin were incubated with 1.5μM of 15% 647-Alexa ATP-actin monomers, 100 nM ATP-Arp2/3 complex, and 500 nM GST-VCA in KMIE buffer for 1 to 2 minutes at 25 °C then immobilized on the neutravidin coated glass surface (*Materials and Methods*). Unbound proteins were washed out with KMIE buffer supplemented with 0.2 μM unlabeled actin monomers, 15 mM glucose, 0.02 mg mL^{-1} catalase, and 0.1 mg mL^{-1} glucose oxidase. In these movies, the filaments were aged for 30 min to form ADP-actin filaments and ADP-Arp2/3 complex then KMIE buffer supplemented with 0.2 μM unlabeled actin monomers, 15 mM glucose, 0.02 mg mL^{-1} catalase, and 0.1 mg mL^{-1} glucose oxidase flow was applied at a constant but variable rate throughout the entire movie. The videos begin after aging and before applying flow (flow rate is specified in each caption). The flow is applied towards the mother filament barbed end direction (bottom to top of the image). In videos S1-3, S6, and S7, the red or magenta portion of the actin filament is immobilized on the surface with biotin whereas the green or cyan portion of the actin filament (mother filament or branch) is freely fluctuating (Fig. 1A). In videos S4 and S5, the entire mother filament is colored red or magenta and the 488-Alexa labeled Arp2/3 complex is colored green or cyan. The scale bars represent 2 μm. The samples are stationary but appear to drift due to imprecise repositioning of the stage as it moved continuously to capture multiple fields of view during the experiments.

Movie S1: Time lapse movies of fluorescence micrographs at 20 s intervals showing dissociation of a branch formed by Arp2/3 complex at time 1680 s with a flow rate of 2 μL min^{-1}, corresponding to a “low” force of ~0.004 pN on a branch 1.5 μm long.

Movie S2: Time lapse movies of fluorescence micrographs at 10 s intervals showing dissociation of a branch formed by Arp2/3 complex at time 1050 s with a flow rate of 50 μL min^{-1}, corresponding to a “medium” force of ~0.10 pN on a branch 1.5 μm long.

Movie S3: Time lapse movies of fluorescence micrographs at 3s intervals showing dissociation of a branch formed by Arp2/3 complex at time 48, 66, 219, and 480 s with a flow rate of 500 μL min^{-1}, corresponding to a “medium” force of ~1.02 pN on a branch 1.5 μm long.

Movie S4 and 5: Time lapse movies of fluorescence micrographs at 100 ms intervals showing dissociation of a branch formed by 488-Alexa labeled snap Arp2/3 complex at approximately 5 s (denoted by the white arrow) with a flow rate of 500 μL min^{-1}, corresponding to a “high” force of ~1.02 pN on a branch 1.5 μm long. Buffer flow is applied after 300 ms, 3 frames.

Movie S6: Time lapse movies of fluorescence micrographs at 3 s intervals showing dissociation of a branch formed by Arp2/3 complex that are aligned with the direction of buffer flow at time 33, 39, 54 s with a flow rate of 500 μL min^{-1}, corresponding to a “high” force of ~1.02 pN on a branch 1.5 μm long.

Movie S7: Time lapse movies of fluorescence micrographs at 3 s intervals showing dissociation of a branch formed by Arp2/3 complex that are aligned against the direction of buffer flow at time 36, 90 s with a flow rate of 500 μL min^{-1}, corresponding to a “high” force of ~1.02 pN on a branch 1.5 μm long.

Part 2. Two-state model for actin network debranching.

Actin network debranching was interpreted using the following branched kinetic pathway model (Scheme S1; Figure 2B) containing two Arp2/3 complex (*Arp*) mechanical states that convert irreversibly with rate constant k_{conv} and dissociate independently from the mother filament (*A*) with rate constants k_1 and k_2:

$$\begin{array}{ccccc} Arp + A & \xrightarrow{k_{form}} & branch_1 & \xrightarrow{k_{conv}} & branch_2 \\ & & \downarrow k_1 & & \downarrow k_2 \\ & & debranched & & \end{array} \qquad \text{Scheme S1}$$

The derivation and analysis presented here were used to determine the rate constants for branch formation (k_{form}), conversion between mechanical state 1 and 2 (k_{conv}), and debranching (k_1 and k_2).

Our experiments were carried out under two distinct force and reaction component regimes: all protein components were mixed together and the branched network was allowed to form for 2.6 min in KMIE buffer containing 2 mM MgATP, after which free unreacted protein and other components (e.g. labeled actin monomer, Arp2/3 complex, GST-VCA and other proteins, as indicated) were washed out by gentle flow of the same KMIE buffer containing 0.2 μM unlabeled actin monomer to prevent filaments from depolymerization. Without free Arp2/3 complex in solution, no additional branches formed after this initial washout. Branched networks were then allowed to further "age" for various times (with gentle flow of 2 μL min^{-1}; force ≈ 0 to minimize any rebinding of dissociating protein components) before applying constant external force with flow.

During filament assembly and aging, polymerized actin hydrolyzes bound ATP with a rate constant of 0.3 sec^{-1} and releases the γ-phosphate slowly (2, 3). Arp2 and Arp3 also hydrolyze bound ATP and dissociate γ-phosphate after branch formation (4, 5). Debranching was observed under flow, so debranched filaments were washed away and branch dissociation was considered to be irreversible. External force can affect k_{conv}, k_1 and/or k_2. Force may also influence branch formation and the value of k_{form}, but we assembled branches in the absence of force.

1) <u>*Minimal model for two Arp2/3 nucleotide branch formation without force during aging time*</u>.
Arp2/3 complex with ATP bound to Arp2 and Arp3 binds actin filaments. Only ~1% of binding events are productive and generate branches (6). We combine reversible Arp2/3 binding and subsequent irreversible branch formation into a single irreversible branch formation step, defined as composite association rate constant k_{form} (Scheme 1). We note that branch formation and dissociation occur through different reaction pathways, rather than a single reversible reaction.

Immediately after branch formation, Arp2/3 complexes are in state 1 ($branch_1$) which we assume is the ADP-P_i state, since ATP hydrolysis is coupled to branch formation ((4), see also (5)). If hydrolysis lags slightly after formation, as with actin (7), $branch_1$ could represent a mixture of ATP and ADP-P_i states. State 1 branches can elongate, dissociate irreversibly with rate constant k_1, or convert to state 2 ($branch_2$) with rate constant k_{conv}. The conversion from state 1 to state 2 is likely associated with P_i release from Arp2/3 complex (discussed in main text). Therefore, the conformation of the Arp2/3 complex in state 1 is considered an ADP-P_i conformation/state, whereas state 2 an ADP conformation/state. Conversion is treated as an (essentially) irreversible transition, given that inclusion of 20 mM P_i has no detectable effects on debranching (Figure S2). This behavior could arise from an irreversible kinetic transition associated with P_i release (since released P_i is washed away and cannot rebind) and/or a weak P_i binding affinity (K_d >> 20 mM).

Given these conditions, the differential equations describing the biochemical reactions depicted in Scheme 1 are given by:

$$\frac{d[branch_1]}{dt} = k_{form}[Arp][A] - \left(k_{conv} + k_1\right)[branch_1]$$
$$= k_{form}[Arp]\left([A]_0 - [branch_1] - [branch_2]\right) - \left(k_{conv} + k_1\right)[branch_1]$$

$$= k_{form}[Arp][A]_0 - \left(k_{form}[arp] + k_{conv} + k_1\right)[branch_1] - k_{form}[Arp][branch_2] \quad \text{S1}$$

and

$$\frac{d[branch_2]}{dt} = k_{conv}[branch_1] - k_2[branch_2], \quad \text{S2,}$$

where $[A]$ is the concentration of filamentous actin available (i.e. free) to bind Arp2/3 complex, while $[A]_0$ is total filamentous actin concentration (free and with bound Arp 2/3 complex). Mass conservation dictates that $[A]_0 = [A] + [branch_1] + [branch_2]$.

The Eigen values of Eqs. S1 and S2 yield two observed rate constants (λ_1 and λ_2) according to:

$$\begin{vmatrix} k_{form}[Arp] + k_{conv} + k_1 - \lambda & k_{form}[Arp] \\ -k_{conv} & k_2 - \lambda \end{vmatrix} = \left(k_{form}[Arp] + k_{conv} + k_1 - \lambda\right)\left(k_2 - \lambda\right) + k_{conv}k_{form}[Arp] \quad \text{S3,}$$

And its characteristic equation is

$$\lambda^2 - \left(k_{form}[Arp] + k_{conv} + k_1 + k_2\right)\lambda + k_2\left(k_{form}[Arp] + k_{conv} + k_1\right) + k_{conv}k_{form}[Arp] = 0 \quad \text{S4,}$$

The two exponential rate constants ($\lambda_{form,+/-}$) for branch formation are given by:

$$\lambda_{form,\pm} = \frac{1}{2}\left(k_{form}[Arp] + k_{conv} + k_1 + k_2 \right.$$
$$\left. \pm\sqrt{\left(k_{form}[Arp] + k_{conv} + k_1 + k_2\right)^2 - 4\left(k_2\left(k_{form}[Arp] + k_{conv} + k_1\right) + k_{conv}k_{form}[Arp]\right)}\right). \quad \text{S5.}$$

To obtain a constant special solution for the differential equations Eqs. S1 and S2, we let $[branch_1] = C_1$ and $[branch_2] = C_2$ and substitute them into Eqs. S1 and S2 to yield:

$$\frac{dC_1}{dt} + \left(k_{form}[Arp] + k_{conv} + k_1\right)C_1 + k_{form}[Arp]C_2$$
$$= \left(k_{form}[Arp] + k_{conv} + k_1\right)C_1 + k_{form}[Arp]C_2 = k_{form}[Arp][A]_0$$
$$-k_2C_1 + \frac{dC_2}{dt} + k_2C_2 = -k_2C_1 + k_2C_2 = 0 \quad \text{S6.}$$

The solution to these differential equations is given by:

$$C_1 = \frac{\begin{vmatrix} k_{form}[Arp][A]_0 & k_{form}[Arp] \\ 0 & k_2 \end{vmatrix}}{\begin{vmatrix} k_{form}[Arp] + k_{conv} + k_1 & k_{form}[Arp] \\ -k_{conv} & k_2 \end{vmatrix}} = \frac{k_2k_{form}[Arp][A]_0}{k_2\left(k_{form}[arp] + k_{conv} + k_1\right) + k_{conv}k_{form}[Arp]} \quad \text{S7}$$

and

$$C_2 = \frac{\begin{vmatrix} k_{form}[Arp] + k_{conv} + k_1 & k_{form}[Arp][A]_0 \\ -k_{conv} & 0 \end{vmatrix}}{\begin{vmatrix} k_{form}[Arp] + k_c + k_1 & k_{form}[Arp] \\ -k_{conv} & k_2 \end{vmatrix}} = \frac{k_ck_{form}[Arp][A]_0}{k_2\left(k_{form}[Arp] + k_{conv} + k_1\right) + k_{conv}k_{form}[Arp]} \quad \text{S8.}$$

Eqs. S1 and S2 have the following general solution:

$$\begin{pmatrix}[branch_1]\\ [branch_2]\end{pmatrix} = A_{form,+}\begin{pmatrix}1\\ \dfrac{k_{conv}}{k_2-\lambda_{form,+}}\end{pmatrix}e^{-\lambda_{form,+}t} + A_{form,-}\begin{pmatrix}1\\ \dfrac{k_{conv}}{k_2-\lambda_{form,-}}\end{pmatrix}e^{-\lambda_{form,-}t}$$
$$+\frac{k_{form}[Arp][A]_0}{k_2\left(k_{form}[Arp]+k_{conv}+k_1\right)+k_{conv}k_{form}[Arp]}\begin{pmatrix}k_2\\ k_{conv}\end{pmatrix}$$
$$= A_{form,+}\begin{pmatrix}1\\ \dfrac{k_{conv}}{k_2-\lambda_{form,+}}\end{pmatrix}e^{-\lambda_{form,+}t} + A_{form,-}\begin{pmatrix}1\\ \dfrac{k_{conv}}{k_2-\lambda_{form,-}}\end{pmatrix}e^{-\lambda_{form,-}t} + q\begin{pmatrix}k_2\\ k_{conv}\end{pmatrix} \quad \text{S9,}$$

where the constant q in the third term is defined as

$$q = \frac{k_{form}[Arp][A]_0}{k_2\left(k_{form}[Arp]+k_{conv}+k_1\right)+k_{conv}k_{form}[Arp]} \quad \text{S10.}$$

$A_{form,+}$ and $A_{form,-}$ in Eq. S9 are arbitrary amplitude constants that depend on the branch concentration and thus, protein concentration. We assume that no branches exist at $t = 0$:

$$\left.\begin{pmatrix}[branch_1]\\ [branch_2]\end{pmatrix}\right|_{t=0} = A_{form,+}\begin{pmatrix}1\\ \dfrac{k_{conv}}{k_2-\lambda_{form,+}}\end{pmatrix} + A_{form,-}\begin{pmatrix}1\\ \dfrac{k_{conv}}{k_2-\lambda_{form,-}}\end{pmatrix} + q\begin{pmatrix}k_2\\ k_{conv}\end{pmatrix}$$
$$= \begin{pmatrix}A_{form,+}+A_{form,-}+k_2 q\\ \dfrac{A_{form,+}k_{conv}}{k_2-\lambda_{form,+}} + \dfrac{A_{form,-}k_{conv}}{k_2-\lambda_{form,-}} + k_c q\end{pmatrix} = \begin{pmatrix}0\\ 0\end{pmatrix} \quad \text{S11.}$$

Solving Eq. S11, the constants are given by the following:

$$A_{+\,form,} = q\frac{\begin{vmatrix}-k_2 & 1\\ -1 & \dfrac{1}{k_2-\lambda_{form,-}}\end{vmatrix}}{\begin{vmatrix}1 & 1\\ \dfrac{1}{k_2-\lambda_{form,+}} & \dfrac{1}{k_2-\lambda_{form,-}}\end{vmatrix}} = q\frac{-\dfrac{k_2}{k_2-\lambda_{form,-}}+1}{\dfrac{1}{k_2-\lambda_{form,-}}-\dfrac{1}{k_2-\lambda_{form,+}}} = q\frac{-\lambda_{form,-}\left(k_2-\lambda_{form,+}\right)}{-\lambda_{form,+}+\lambda_{form,-}} \quad \text{S12,}$$

and

$$A_{form,-} = q\frac{\begin{vmatrix} 1 & -k_2 \\ \dfrac{1}{k_2-\lambda_{form,+}} & -1 \end{vmatrix}}{\begin{vmatrix} 1 & 1 \\ \dfrac{1}{k_2-\lambda_{form,+}} & \dfrac{1}{k_2-\lambda_{form,-}} \end{vmatrix}} = q\frac{-1+\dfrac{k_2}{k_2-\lambda_{form,+}}}{\dfrac{1}{k_2-\lambda_{form,-}}-\dfrac{1}{k_2-\lambda_{form,+}}} = q\frac{\lambda_{form,+}\left(k_2-\lambda_{form,-}\right)}{-\lambda_{form,+}+\lambda_{form,-}} \quad \text{S13,}$$

and the solution to Eq. S9 is given by:

$$\begin{pmatrix}[branch_1]\\ [branch_2]\end{pmatrix} = q\frac{-\lambda_{form,-}\left(k_2-\lambda_{form,+}\right)}{-\lambda_{form,+}+\lambda_{form,-}}\begin{pmatrix}1\\ \dfrac{k_{conv}}{k_2-\lambda_{form,+}}\end{pmatrix}e^{-\lambda_{form,+}t}$$

$$+q\frac{\lambda_{form,+}\left(k_2-\lambda_{form,-}\right)}{-\lambda_{form,+}+\lambda_{form,-}}\begin{pmatrix}1\\ \dfrac{k_{conv}}{k_2-\lambda_{form,-}}\end{pmatrix}e^{-\lambda_{form,-}t}+q\begin{pmatrix}k_2\\ k_{conv}\end{pmatrix}$$

$$=q\begin{pmatrix}-\dfrac{\lambda_{form,-}\left(k_2-\lambda_{form,+}\right)}{-\lambda_{form,+}+\lambda_{form,-}}e^{-\lambda_{form,+}t}+\dfrac{\lambda_{form,+}\left(k_2-\lambda_{form,-}\right)}{-\lambda_{form,+}+\lambda_{form,-}}e^{-\lambda_{form,-}t}+k_2\\ \dfrac{k_{conv}}{-\lambda_{form,+}+\lambda_{form,-}}\left(-\lambda_{form,-}e^{-\lambda_{form,+}t}+\lambda_{form,+}e^{-\lambda_{form,-}t}\right)+k_{conv}\end{pmatrix} \quad \text{S14.}$$

2) *Model for converting between Arp2/3 actin branch nucleotide states under no force during aging.*
After initial branched actin filament network formation, all untethered proteins (free actin, Arp2/3 complex, and GST-VCA) are washed out of the reaction chamber so that no additional branches form. Accordingly, the relevant reaction scheme during the remaining aging time after wash out should be identical to Scheme S1 without the branch formation transition:

$$\begin{array}{ccc} branch_1 & \xrightarrow{k_{conv}} & branch_2 \\ \downarrow k_1 & & \downarrow k_2 \\ debranched & & \end{array} \quad \text{Scheme S2}$$

The differential equations describing the reactions in Scheme S2 are:

$$\frac{d[branch_1]}{dt} = -\left(k_1+k_{conv}\right)[branch_1] \quad \text{S15}$$

$$\frac{d[branch_2]}{dt} = k_{conv}[branch_1]-k_2[branch_2] \quad \text{S16.}$$

Note that the differential equation accounting for *branch*$_2$ formation (Eq. S16) following Scheme S2 is identical to that obtained according to Scheme S1 (Eq. S2).

Differential equation Eq. S15 can be directly integrated to yield:

$$[branch_1] = [branch_1]_{t_1}e^{-(k_{conv}+k_1)(t-t_1)} \quad \text{S17,}$$

where $[branch_1]_{t_1}$ is the concentration of branches in the *branch*$_1$ state formed during time t_1. Substituting Eq. S17 into Eq. S16 yields

$$\frac{d[branch_2]}{dt} + k_2[branch_2] = k_{conv}[branch_1]_{t_1} e^{-(k_{conv}+k_1)(t-t_1)} \quad \text{S18.}$$

Using the variation of parameter method, a general solution of this inhomogeneous differential equation (Eq. S18) can be obtained. When $k_2 \neq k_1 + k_{conv}$:

$$[branch_2] = \frac{k_{conv}[branch_1]_{t_1}}{k_2 - k_1 - k_{conv}} e^{-(k_1+k_{conv})(t-t_1)} + Ce^{-k_2(t-t_1)}, \quad k_2 \neq k_1 + k_{conv} \quad \text{S19,}$$

and when $k_2 = k_1 + k_{conv}$:

$$[branch_2] = \left(k_{conv}[branch_1]_{t_1} t + C\right) e^{-k_2(t-t_1)}, \quad k_2 = k_1 + k_{conv} \quad \text{S20.}$$

Eqs. S17, S19 and S20 show that when $k_2 \neq k_1 + k_{conv}$, the debranching process has two exponential phases (given by Eqs. S17 and S19) with observed rate constants ($k_{obs,1}$ and $k_{obs,2}$) defined by ($k_1 + k_{conv}$) and k_2, respectively. When $k_2 = k_1 + k_{conv}$, the debranching process is sum of a single exponential ($k_{obs} = (k_1 + k_{conv})$ or k_2) and a non-exponential phase (Eqs. S17 and S20).

The arbitrary constant C in Eqs. S19 and S20 is determined by the populations of $branch_1$ and $branch_2$ formed during formation time t_1. When $t = t_1$, the constant C in Eqs. S19 and S20 is given by:

$$C = [branch_2]_{t_1} - \frac{k_{conv}[branch_1]_{t_1}}{k_2 - k_1 - k_{conv}}, \quad k_2 \neq k_1 + k_{conv} \quad \text{S21}$$

or

$$C = [branch_2]_{t_1} - k_{conv}[branch_1]_{t_1} t_1, \quad k_2 = k_1 + k_{conv} \quad \text{S22.}$$

Substituting of Eq. S21 or S22 into Eq. S19 or S20 generates:

$$[branch_2] = \frac{k_{conv}[branch_1]_{t_1}}{k_2 - k_1 - k_{conv}} e^{-(k_1+k_{conv})(t-t_1)} + \left([branch_2]_{t_1} - \frac{k_{conv}[branch_1]_{t_1}}{k_2 - k_1 - k_{conv}}\right) e^{-k_2(t-t_1)} \quad \text{S23}$$

$$k_2 \neq k_1 + k_{conv}$$

and

$$[branch_2] = \left(k_{conv}[branch_1]_{t_1} t + [branch_2]_{t_1} - k_{conv}[branch_1]_{t_1} t_1\right) e^{-k_2(t-t_1)}$$

$$= \left(k_{conv}[branch_1]_{t_1} (t - t_1) + [branch_2]_{t_1}\right) e^{-k_2(t-t_1)}, \quad k_2 = k_1 + k_{conv} \quad \text{S24.}$$

Therefore, the time dependent total combined branches in two states is the sum of Eqs. S17 and S23 or S24

$$[branch_1] + [branch_2] = [branch_1]_{t_1} e^{-(k_{conv}+k_1)(t-t_1)} + \frac{k_{conv}[branch_1]_{t_1}}{k_2 - k_1 - k_{conv}} e^{-(k_1+k_{conv})(t-t_1)}$$

$$+ \left([branch_2]_{t_1} - \frac{k_{conv}[branch_1]_{t_1}}{k_2 - k_1 - k_{conv}}\right) e^{-k_2(t-t_1)}$$

$$= \frac{(k_2 - k_1)[branch_1]_{t_1}}{k_2 - k_1 - k_{conv}} e^{-(k_1+k_{conv})(t-t_1)} + \left([branch_2]_{t_1} - \frac{k_{conv}[branch_1]_{t_1}}{k_2 - k_1 - k_{conv}}\right) e^{-k_2(t-t_1)} \quad \text{S25}$$

$$k_2 \neq k_1 + k_{conv}$$

or

$$[branch_1] + [branch_2] = [branch_1]_{t_1} e^{-(k_{conv}+k_1)(t-t_1)} + \left(k_{conv}[branch_1]_{t_1} (t - t_1) + [branch_2]_{t_1}\right) e^{-k_2(t-t_1)} \quad \text{S26.}$$

$$k_2 = k_1 + k_{conv}$$

If $k_1 \sim k_2$, the first exponential term in Eq. 25 disappears and the combined total branches of two states follow a single exponential decay (see below).

3) *Model for Arp2/3 actin branches debranching under force after aging*.
After a defined aging time t_{age} (accounted in the two preceding sections), dynamic flow was introduced to exert drag force on branches. The applicable reaction scheme under these experimental conditions is identical to that illustrated in Scheme S2, but with all rate constants replaced with ones under force (k_1, k_2 and k_{conv} become $k_{1,F}$, $k_{2,F}$ and $k_{conv,F}$). Accordingly, debranching under force follows the equations in the same form as Eqs. S17 and S23:

$$[branch_1]_F = [branch_1]_{F,0} e^{-(k_{conv,F}+k_{1,F})t} \quad \text{S27}$$

$$[branch_2]_F = \frac{k_{conv,F}[branch_1]_{F,0}}{k_{2,F}-k_{1,F}-k_{conv,F}} e^{-(k_{1,F}+k_{conv,F})t} + \left([branch_2]_{F,0} - \frac{k_{conv,F}[branch_1]_{F,0}}{k_{2,F}-k_{1,F}-k_{conv,F}} \right) e^{-k_{2,F}t} \quad \text{S28.}$$

$$k_{2,F} \neq k_{1,F} + k_{conv,F}$$

Because time courses of debranching under force follow a sum of exponentials, we can eliminate the solution with $k_{2,F} = k_{1,F} + k_{conv,F}$ (S24) since this has a non-exponential term in it that is not observed in the experimental data.

Time courses of observed debranching under force is given by sum of debranching from the both Arp2/3 complex branch states:

$$\begin{aligned}[branch]_F &= [branch_1]_{F,0} e^{-(k_{conv,F}+k_{1,F})t} + \frac{k_{conv,F}[branch_1]_{F,0}}{k_{2,F}-k_{1,F}-k_{conv,F}} e^{-(k_{1,F}+k_{conv,F})t} \\ &+ \left([branch_2]_{F,0} - \frac{k_{c,F}[branch_1]_{F,0}}{k_{2,F}-k_{1,F}-k_{conv,F}} \right)_F e^{-k_{2,F}t} \\ &= \frac{(k_{2,F}-k_{1,F})[branch_1]_{F,0}}{k_{2,F}-k_{1,F}-k_{conv,F}} e^{-(k_{1,F}+k_{conv,F})t} + \left([branch_2]_{F,0} - \frac{k_{conv,F}[branch_1]_{F,0}}{k_{2,F}-k_{1,F}-k_{conv,F}} \right) e^{-k_{2,F}t} \end{aligned} \quad \text{S29.}$$

Time courses of debranching follow double exponentials with slow (s) and fast (f) observed rate constants (k_s and k_f) equal to ($k_{1,F} + k_{conv,F}$) and $k_{2,F}$. The experimental data shows that aging accelerates branch dissociation (Figure 3). Therefore, fast dissociation occurs late in Scheme S2 and $k_s = (k_{1,F} + k_{conv,F})$ and $k_f = k_{2,F}$.

We define $[branch_1]_{F,0}$ and $[branch_2]_{F,0}$ as initial branch populations (formed during aging in the absence of force) the moment that force is applied. According to Eqs S17 and S23 or S24, the initial branch populations in Eqs. S27 and S28 become:

$$[branch_1]_{F,0} = [branch_1]_{t_1} e^{-(k_{conv,F}+k_1)(t_{age}-t_1)} \quad \text{S30}$$

$$[branch_2]_{F,0} = \frac{k_c[branch_1]_{t_1}}{k_2-k_1-k_{conv,F}} e^{-(k_1+k_{conv,F})(t_{age}-t_1)} + \left([branch_2]_{t_1} - \frac{k_{conv,F}[branch_1]_{t_1}}{k_2-k_1-k_{conv,F}} \right) e^{-k_2(t_{age}-t_1)} \quad \text{S31}$$

$$k_2 \neq k_1 + k_{conv,F}$$

or

$$[branch_2]_{F,0} = \left(k_{conv,F}[branch_1]_{t_1}(t_{age}-t_1) + [branch_2]_{t_1} \right) e^{-k_2(t_{age}-t_1)}, \quad k_2 = k_1 + k_{conv,F} \quad \text{S32,}$$

where t_{age} is time of branching formation and subsequent aging.

The fractional amplitude of the slow $A_{s,F}$ (exponential) debranching phase under force is given by according to Eq. 29:

$$A_{s,F} = \frac{\frac{\left(k_{2,F} - k_{1,F}\right)[branch_1]_{F,0}}{k_{2,F} - k_{1,F} - k_{conv,F}}}{[branch_1]_{F,0} + [branch_2]_{F,0}} \qquad \text{S33}$$

which can be rewritten as:

$$= \frac{\frac{k_{2,F} - k_{1,F}}{k_{2,F} - k_{1,F} - k_{conv,F}}[branch_1]_{t_1} e^{-(k_{conv}+k_1)(t_{age}-t_1)}}{[branch_1]_{t_1} e^{-(k_{conv}+k_1)(t_{age}-t_1)} + \frac{k_{conv}[branch_1]_{t_1}}{k_2 - k_1 - k_{conv}} e^{-(k_1+k_{conv})(t_{age}-t_1)} + \left([branch_2]_{t_1} - \frac{k_{conv}[branch_1]_{t_1}}{k_2 - k_1 - k_{conv}}\right) e^{-k_2(t_{age}-t_1)}}$$

$$= \frac{\frac{k_{2,F} - k_{1,F}}{k_{2,F} - k_{1,F} - k_{conv,F}} e^{-(k_{conv}+k_1)(t_{age}-t_1)}}{\frac{k_2 - k_1}{k_2 - k_1 - k_{conv}} e^{-(k_1+k_{conv})(t_{age}-t_1)} + \left(\frac{[branch_2]_{t_1}}{[branch_1]_{t_1}} - \frac{k_{conv}}{k_2 - k_1 - k_{conv}}\right) e^{-k_2(t_{age}-t_1)}}$$

$$= \frac{\frac{\frac{k_{2,F} - k_{1,F}}{k_{2,F} - k_{1,F} - k_{conv,F}}}{\frac{[branch_2]_{t_1}}{[branch_1]_{t_1}} - \frac{k_{conv}}{k_2 - k_1 - k_{conv}}} e^{-(k_{conv}+k_1-k_2)(t_{age}-t_1)}}{1 + \frac{\frac{k_2 - k_1}{k_2 - k_1 - k_{conv}}}{\frac{[branch_2]_{t_1}}{[branch_1]_{t_1}} - \frac{k_{conv}}{k_2 - k_1 - k_{conv}}} e^{-(k_1+k_{conv}-k_2)(t_{age}-t_1)}} = \frac{be^{-(k_{conv}+k_1-k_2)(t_{age}-t_1)}}{1 + ae^{-(k_1+k_{conv}-k_2)(t_{age}-t_1)}}, \quad k_2 \neq k_1 + k_{conv} \qquad \text{S34}$$

when $k_2 \neq k_1 + k_{conv}$, and

$$= \frac{\frac{k_{2,F} - k_{1,F}}{k_{2,F} - k_{1,F} - k_{conv,F}}[branch_1]_{t_1} e^{-(k_{conv}+k_1)(t_{age}-t_1)}}{[branch_1]_{t_1} e^{-(k_{conv}+k_1)(t_{age}-t_1)} + \left(k_{conv}[branch_1]_{t_1}\left(t_{age} - t_1\right) + [branch_2]_{t_1}\right) e^{-k_2(t_{age}-t_1)}}$$

$$= \frac{\frac{k_{2,F} - k_{1,F}}{k_{2,F} - k_{1,F} - k_{conv,F}}}{\left(1 + \frac{[branch_2]_{t_1}}{[branch_1]_{t_1}} - k_{conv}t_1\right) + k_{conv}t_{age}} = \frac{1}{b' + a't_{age}}, \quad k_2 = k_1 + k_{conv} \qquad \text{S35}$$

when $k_2 = k_1 + k_{conv}$.

The fractional amplitude of the fast $A_{f,F}$ debranching phase under force is given by:

$$A_{f,F} = \frac{[branch_2]_{F,0} - \frac{k_{conv,F}[branch_1]_{F,0}}{k_{2,F} - k_{1,F} - k_{conv,F}}}{[branch_1]_{F,0} + [branch_2]_{F,0}} \qquad \text{S36}$$

which can be rewritten as

$$
\begin{aligned}
&\frac{k_{conv}[branch_1]_{t_1}}{k_2-k_1-k_{conv}}e^{-(k_1+k_{conv})(t_{age}-t_1)}+\left([branch_2]_{t_1}-\frac{k_{conv}[branch_1]_{t_1}}{k_2-k_1-k_{conv}}\right)e^{-k_2(t_{age}-t_1)}\\
&=\frac{-\dfrac{k_{conv,F}}{k_{2,F}-k_{1,F}-k_{conv,F}}[branch_1]_{t_1}e^{-(k_{conv}+k_1)(t_{age}-t_1)}}{\dfrac{k_2-k_1}{k_2-k_1-k_{conv}}[branch_1]_{t_1}e^{-(k_1+k_{conv})(t_{age}-t_1)}+\left([branch_2]_{t_1}-\dfrac{k_{conv}[branch_1]_{t_1}}{k_2-k_1-k_{conv}}\right)e^{-k_2(t_{age}-t_1)}}\\
&=\frac{1+\dfrac{\dfrac{k_{conv}}{k_2-k_1-k_{conv}}-\dfrac{k_{conv,F}}{k_{2,F}-k_{1,F}-k_{conv,F}}}{\dfrac{[branch_2]_{t_1}}{[branch_1]_{t_1}}-\dfrac{k_{conv}}{k_2-k_1-k_{conv}}}e^{-(k_{conv}+k_1-k_2)(t_{age}-t_1)}}{1+\dfrac{\dfrac{k_2-k_1}{k_2-k_1-k_{conv}}}{\dfrac{[branch_2]_{t_1}}{[branch_1]_{t_1}}-\dfrac{k_{conv}}{k_2-k_1-k_{conv}}}e^{-(k_1+k_{conv}-k_2)(t_{age}-t_1)}}\\
&=\frac{1+\dfrac{\dfrac{k_2-k_1}{k_2-k_1-k_{conv}}-\dfrac{k_{2,F}-k_{1,F}}{k_{2,F}-k_{1,F}-k_{conv,F}}}{\dfrac{[branch_2]_{t_1}}{[branch_1]_{t_1}}-\dfrac{k_{conv}}{k_2-k_1-k_{conv}}}e^{-(k_{conv}+k_1-k_2)(t_{age}-t_1)}}{1+\dfrac{\dfrac{k_2-k_1}{k_2-k_1-k_{conv}}}{\dfrac{[branch_2]_{t_1}}{[branch_1]_{t_1}}-\dfrac{k_{conv}}{k_2-k_1-k_{conv}}}e^{-(k_1+k_{conv}-k_2)(t_{age}-t_1)}}\\
&=\frac{1+(a-b)e^{-(k_{conv}+k_1-k_2)(t_{age}-t_1)}}{1+ae^{-(k_1+k_{conv}-k_2)(t_{age}-t_1)}}=1-A_{s,F},\quad k_2\neq k_1+k_{conv}
\end{aligned}
\tag{S37}
$$

when $k_2 \neq k_1 + k_{conv}$, and

$$
\begin{aligned}
&\frac{\left(k_{conv}[branch_1]_{t_1}(t_{age}-t_1)+[branch_2]_{t_1}\right)e^{-k_2(t_{age}-t_1)}-\dfrac{k_{conv,F}}{k_{2,F}-k_{1,F}-k_{conv,F}}[branch_1]_{t_1}e^{-(k_{conv}+k_1)(t_{age}-t_1)}}{[branch_1]_{t_1}e^{-(k_{conv}+k_1)(t_{age}-t_1)}+\left(k_{conv}[branch_1]_{t_1}(t_{age}-t_1)+[branch_2]_{t_1}\right)e^{-k_2(t_{age}-t_1)}}\\
&=\frac{\dfrac{[branch_2]_{t_1}}{[branch_1]_{t_1}}-\dfrac{k_{conv,F}}{k_{2,F}-k_{1,F}-k_{conv,F}}-k_{conv}t_1+k_{conv}t_{age}}{1+\dfrac{[branch_2]_{t_1}}{[branch_1]_{t_1}}-k_{conv}t_1+k_{conv}t_{age}}\\
&=\frac{b'-1+a't_{age}}{b'+a't_{age}}=1-\frac{1}{b'+a't_{age}}=1-A_{s,F},\quad k_2=k_1+k_{conv}
\end{aligned}
\tag{S38}
$$

when $k_2 = k_1 + k_{conv}$. Eqs. S35 and S38 indicate that when $k_2 = k_1 + k_{conv}$, the fractional fast and slow amplitudes depend hyperbolically on the age time (t_{age}).

In the above equations, the constants a, a', b, and b' are defined by:

$$a = \frac{\dfrac{k_2 - k_1}{k_2 - k_1 - k_{conv}}}{\dfrac{[branch_2]_{t_1}}{[branch_1]_{t_1}} - \dfrac{k_{conv}}{k_2 - k_1 - k_{conv}}}, \quad b = \frac{\dfrac{k_{2,F} - k_{1,F}}{k_{2,F} - k_{1,F} - k_{conv,F}}}{\dfrac{[branch_2]_{t_1}}{[branch_1]_{t_1}} - \dfrac{k_{conv}}{k_2 - k_1 - k_{conv}}} \qquad \text{S39}$$

$$a' = \frac{k_{conv}}{\dfrac{k_{2,F} - k_{1,F}}{k_{2,F} - k_{1,F} - k_{conv,F}}}, \quad b' = \frac{1 + \dfrac{[branch_2]_{t_1}}{[branch_1]_{t_1}} - k_{conv} t_1}{\dfrac{k_{2,F} - k_{1,F}}{k_{2,F} - k_{1,F} - k_{conv,F}}} \qquad \text{S40.}$$

4) *Determination of the branch formation, conversion, and debranching rate constants in the absence of force*. Global fitting of the aging time-dependent time courses of debranching under force to a double exponential equation (Fig. 2B) yielded slow ($k_{s,F}$) and fast ($k_{f,F}$) phase observed rate constants, expressed as slow and fast lifetimes ($\tau = 1/k_{obs}$), values of $\tau_{s,F} = 3.08 \pm 0.05$ and $\tau_{f,F} = 0.15 \pm 0.01$ min. According to Eq. S29, the corresponding rate constants are given by:

$$k_{s,F} = k_{1,F} + k_{conv,F} = \frac{1}{\tau_s} = 0.32 \pm 0.005 \text{ min}^{-1}$$
$$k_{f,F} = k_{2,F} = \frac{1}{\tau_f} = 6.67 \pm 0.44 \text{ min}^{-1} \qquad \text{S41.}$$

The amplitudes from the double exponential fit reflect the distribution between the two Arp2/3 branch states ($branch_1$ and $branch_2$) populated during aging in the absence of force, as described by Eqs. S34 and S37.

Global analysis of the aging time-dependence of the slow and fast phase amplitudes using Eqs. S34 and S37 (Eq. 2 in main text), and the branch formation time $t_1 = 2.6$ min yielded the following parameters in the absence of force (Fig. 4C):

$$k_1 + k_{conv} - k_2 = 0.14 \pm 0.03 \text{ min}^{-1}$$
$$a = 0.01 \pm 0.12 \qquad \text{S42.}$$
$$b = 2.0 \pm 0.4$$

When the aging time equals the branch formation time, i.e., $t_{age} = t_1$, the fractional amplitudes for debranching under force are $A_{s,F} \sim 1$ and $A_{f,F} \sim 0$ (Fig. 4C). According to Eqs. S33 and S36 , the fractional amplitudes of the slow and fast phases at $t_{age} = t_1$ are:

$$A_{s,F}\left(t_{age} = t_1\right) = \frac{\dfrac{\left(k_{2,F} - k_{1,F}\right)[branch_1]_{t_1}}{k_{2,F} - k_{1,F} - k_{conv,F}}}{[branch_1]_{t_1} + [branch_2]_{t_1}} \sim 1 \qquad \text{S43}$$

$$A_{f,F}\left(t_{age} = t_1\right) = \frac{[branch_2]_{t_1} - \dfrac{k_{conv,F}}{k_{2,F} - k_{1,F} - k_{conv,F}}[branch_1]_{t_1}}{[branch_1]_{t_1} + [branch_2]_{t_1}} \sim 0 \qquad \text{S44.}$$

The ratio of the two branch states formed during the initial branch formation time is given by:

$$\frac{[branch_2]_{t_1}}{[branch_1]_{t_1}} \sim \frac{k_{conv,F}}{k_{2,F} - k_{1,F} - k_{conv,F}} < \frac{k_{conv,F} + k_{1,F}}{k_{2,F} - k_{1,F} - k_{conv,F}} \sim 0.05 \qquad \text{S45,}$$

as estimated from the experimentally determined rate constants under force (Eq. S41). Therefore, $[branch_2] \sim 0$ upon conclusion of branch formation time t_1. That is, little or no conversation occurs within the first 2.6 min of

aging and most (>95%) of branches remain in the $branch_1$ state. Given this value and Eq. S39 with the experimental value $a = 0.01$ (S42),

$$a = \frac{\dfrac{k_2 - k_1}{k_2 - k_1 - k_{conv}}}{\dfrac{[branch_2]_{t_1}}{[branch_1]_{t_1}} - \dfrac{k_{conv}}{k_2 - k_1 - k_{conv}}} \sim -\frac{k_2 - k_1}{k_{conv}} = 0.01 \qquad \text{S46.}$$

According to Eq. S46 and the rate constant in Eq. S42, the calculated value of k_{conv} is:

$$k_{conv} = \frac{0.14}{1.01} \sim 0.14 \pm 0.03 \text{ min}^{-1} \qquad \text{S47.}$$

The standard deviation for k_{conv} calculated according to error propagation:

$$\delta k_{conv} = \sqrt{\frac{\delta r^2}{(1+a)^2} + \frac{r^2 \delta a^2}{(1+a)^4}} \qquad \text{S48,}$$

where r is ($k_1 + k_{conv} - k_2$) in the absence of force, and the standard errors $\delta r = 0.03$ and $\delta a = 0.12$ (Eq. S42).

Since the conversion rate constant $k_{conv} = 0.14$ min^{-1} (lifetime for conversion ~ 7 min), conversion from state 1 to state 2 is nearly complete within 30 min age time. This is why time courses of debranching after 30 min aging follow single exponential.

Given this value of k_{conv} value and Eq. S42, yields $k_1 - k_2 \sim 0.0014$ min^{-1} ~ 0 min^{-1}, indicating that $k_1 \sim k_2$, with k_1 slightly larger than k_2. The lifetime of debranching in the absence of force estimated from the force-dependence of debranching after 30 min aging (Fig. 2D) is 106 (± 8) min ($k_{obs} = 0.01 \pm 0.007$ min^{-1}). Since conversion from state 1 to state 2 is completed within 30 min, debranching after a 30 min age time occurs exclusively from state 2. Accordingly, this k_{obs} reflects debranching from state 2 ($k_2 = 0.01 \pm 0.007$ min^{-1}; Table 1). The rate constant for debranching from state 1 in the absence of force is estimated to be $k_1 \sim 0.011$ min^{-1}. Since $k_1 \sim k_2$, the fast exponential term amplitude in the observed debranching time course under no force (Eq. S25) is ~ 0 and the time course reduce to a single exponential decay.

Eq. S4 above represents the rate constant for branch formation during the initial branch formation age time t_1. Since k_1 and k_2 are small compared to both k_{conv} and $k_{form}[Arp]$, the two observed rate constants in Eq. S4 can be approximated as:

$$\lambda_{form,+} = k_{form}[Arp], \quad \lambda_{form,-} = k_{conv} \qquad \text{S49.}$$

During the branch formation time t_1 of 2.6 min, $[branch_2] \sim 0$ (Eq. S14), yields

$$\frac{k_{conv}}{-\lambda_{form,+} + \lambda_{form,-}} \left(-\lambda_{form,-} e^{-\lambda_{form,+} t_1} + \lambda_{form,+} e^{-\lambda_{form,-} t_1} \right) + k_{conv} \sim 0 \qquad \text{S50,}$$

which can be rearranged to:

$$\frac{1 - e^{-\lambda_{form,-} t_1}}{\lambda_{form,-}} = \frac{1 - e^{-\lambda_{form,+} t_1}}{\lambda_{form,+}} \qquad \text{S51.}$$

Assuming $\lambda_{form,+}\, t_1 << 1$ or $t_1 << 1/\lambda_{form,+}$, a Taylor expansion of the exponential function in S51 with $\lambda_{form,+}\, t_1$ to 2nd order yields:

$$= \frac{1-\left(1-\lambda_{form,+}t_1+\frac{1}{2}\lambda_{form,+}{}^2t_1{}^2+O\left(\lambda_{form,+}{}^3t_1{}^3\right)\right)}{\lambda_{form,+}}$$

$$= t_1-\frac{1}{2}\lambda_{form,+}t_1{}^2+O\left(\lambda_{form,+}{}^2t_1{}^3\right) \quad \text{S52.}$$

Given t_1 = 2.6 min and $\lambda_{form,-} \sim k_{conv}$ values (Eq. S49), solving Eq. S51-52 yields

$$\lambda_{form,+} = k_{form}[Arp] = 2\left(\frac{1}{t_1}-\frac{1-e^{-\lambda_{form,-}t_1}}{t_1{}^2\lambda_{form,-}}\right) = 2\left(\frac{1}{t_1}-\frac{1-e^{-k_{conv}t_1}}{t_1{}^2k_{conv}}\right) = 0.12 \text{ min}^{-1} \quad \text{S53.}$$

Debranching experiments were carried out with 0.1 μM Arp2/3. Therefore, the of 2nd order association rate constant for branch formation, $k_{form} = \lambda_{form,+}/[Arp]$ = 1.2 μM^{-1} min^{-1} = 0.02 μM^{-1} sec^{-1}. This rate constant reflects a composite of Arp2/3 binding and subsequent branch formation.

Using the two observed rate constants (Eqs. S47, S49 and S53) for branch formation in Eq. S14, time course of branch formation in the absence of force during time t_1 follow single exponentials and can be constructed from:

$$[branch] = [branch_1]+[branch_2]$$

$$= q\left(-\frac{\lambda_{form,-}\left(k_2-\lambda_{form,+}\right)}{-\lambda_{form,+}+\lambda_{form,-}}e^{-\lambda_{from,+}t}+\frac{\lambda_{form,+}\left(k_2-\lambda_{form,-}\right)}{-\lambda_{form,+}+\lambda_{form,-}}e^{-\lambda_{form,-}t}+k_2\right.$$

$$\left.\frac{k_{conv}}{-\lambda_{form,+}+\lambda_{form,-}}\left(-\lambda_{form,-}e^{-\lambda_{form,+}t}+\lambda_{form,+}e^{-\lambda_{form,-}t}\right)+k_{conv}\right)$$

$$= qk_{conv}\left(1-e^{-\lambda_{from,+}t}\right) \quad \text{S54,}$$

where $k_2 \sim 0$ and $\lambda_{form,-} \sim k_{conv}$.

Part 3. A model for the distribution of branches at the leading edge of cells based on the dependence of the rates of branch dissociation on age and applied force.

The model

We present a minimal kinetic model to assess how the effects of aging, force and GMF on dissociation of branches formed by Arp2/3 complex might explain density of actin filament branches at the leading edge of a motile cell or equivalent situations as a *Listeria* comet tail; Fig. S9). The model assumes (a) that branches form from ATP-Arp2/3 complex only at the leading edge (8), where nucleation promoting factors activate Arp2/3 complex (b) hydrolysis of ATP rapidly converts to Arp2/3 complex in branches to ADP-P_i followed by slow phosphate dissociation, (c) force applied at the leading edge membrane is uniformly distributed throughout the filament network, and (d) the whole network migrates by retrograde flow perpendicular to the cell membrane at the leading edge (i.e. towards the cell interior; Fig. S9) at a constant velocity (v) that is *relative* to and independent of leading edge movement. To an observer, the leading edge is on a *y*-*z* plane at $x = 0$, while the network migrates in the *x*-axis direction by retrograde flow towards the cell interior (Fig. S9). The branches in any efficiently small volume ΔV (Fig. S9, black cube) within the network dissociate as the volume move away from the initial position at the leading edge.

Branches formed by Arp2/3 complex dissociate by two pathways (Scheme S2 above repeated here for convenience):

$$\begin{array}{ccc} branch_1 & \xrightarrow{k_{conv,F}} & branch_2 \\ \downarrow k_{1,F} & & \downarrow k_{2,F} \\ & debranched & \end{array} \qquad \text{Scheme S2,}$$

where $branch_1$ has ADP-P_i bound to Arp2/3 complex, $branch_2$ has ADP bound to Arp2/3 complex, $k_{1,F}$ is the dissociation rate constant for branches with ADP-P_i-Arp2/3 complex, $k_{2,F}$ is the dissociation rate constant for branches with ADP-Arp2/3 complex, and $k_{conv,F}$ is the rate constant for conversion of Arp2/3 complex from the ADP-P_i to ADP state. Force can influence all three rate constants. In this model the distribution of branches is uniform along the *y*- and *z*- directions (i.e. uniform in any *y*-*z* plane along the *x*-axis), but varies along *x*-axis due to branch dissociation. In the absence of force $k_{conv} >> k_1$, so debranching occurs predominately from the branch 2 state and time courses follow single exponentials (Fig. 4B). In the presence of force debranching occurs from both the branch 1 and 2 states.

Branch density distribution

The parallel pathway depicted in Scheme S2 predicts debranching time courses that follow a double exponential decay. Under initial conditions, $t = 0$ and the leading edge, where $[branch_1] = [branch_1]_0$ and $[branch_2] = 0$, the exact solution of Scheme S2 (i.e. the time dependence of the total combined branches in the two states) can be obtained following the same procedure above (from Eq. S15 to S26) as follows:

$$\begin{aligned} &[branch] = [branch_1] + [branch_2] \\ &= [branch_1]_0 e^{-\left(k_{1,F}+k_{conv,F}\right)t} + \frac{k_{conv,F}[branch_1]_0}{k_{2,F}-k_{1,F}-k_{conv,F}}\left(e^{-\left(k_{1,F}+k_{conv,F}\right)t} - e^{-k_{2,F}t}\right) \\ &= \frac{[branch_1]_0}{k_{2,F}-k_{1,F}-k_{conv,F}}\left(\left(k_{2,F}-k_{1,F}\right)e^{-\left(k_{1,F}+k_{conv,F}\right)t} - k_{conv,F}e^{-k_{2,F}t}\right), \quad k_{2,F} \neq k_{1,F}+k_{conv,F} \end{aligned}$$

or

$$\begin{aligned}[branch] &= [branch_1] + [branch_2] \\ &= [branch_1]_0 e^{-\left(k_{1,F}+k_{conv,F}\right)t} + k_{conv,F}[branch_1]_0 te^{-k_{2,F}t} \\ &= [branch_1]_0 \left(1 + k_{conv,F}t\right)e^{-k_{2,F}t}, \quad k_{2,F} = k_{1,F} + k_{conv,F}\end{aligned} \tag{S56}$$

Note that the initial conditions in the derivation Eqs S15-S26 and the solution represented by Eqs. S25 and S26 are slightly different. If $k_{1,F} \sim k_{2,F}$, the first exponential term in Eq. 55 disappears and the combined total branches of two states follow a single exponential decay (see below).

Since the small sample volume (ΔV) travels away from membrane with a constant relative velocity ν in the x direction, the distance from the membrane at time t is $x = \nu t$. Substituting $t = x/\nu$ into Eqs. S55 and S56, yields the spatial distribution of branch concentration in the x-axis direction:

$$[branch] = \frac{[branch_1]_0}{k_{2,F} - k_{1,F} - k_{conv,F}}\left(\left(k_{2,F} - k_{1,F}\right)e^{-\frac{\left(k_{1,F}+k_{conv,F}\right)x}{\nu}} - k_{conv,F}e^{-\frac{k_{2,F}x}{\nu}}\right), \tag{S57}$$

$$k_{2,F} \neq k_{1,F} + k_{conv,F}$$

or

$$[branch] = [branch_1]_0\left(1 + \frac{k_{conv,F}x}{\nu}\right)e^{-\frac{k_{2,F}x}{\nu}}, \quad k_{2,F} = k_{1,F} + k_{conv,F} \tag{S58}$$

In general, when $k_{2,F} \neq k_{1,F} + k_{conv,F}$, the spatial distribution of the branch concentration follows a double exponential decay towards the cell interior with a total amplitude given by the initial branch concentration at the membrane ($[branch_1]_0$). The overall "decay length" of the double exponential decay is discussed below. In a rare, special case, when, when $k_{2,F} = k_{1,F} + k_{conv,F}$, the branch concentration spatial distribution follows a single exponential decay (see also (9-12)) toward the cell interior with additional non-exponential terms. Since this is a rare and special case, we focus our discussion on the general case when $k_{2,F} \neq k_{1,F} + k_{conv,F}$.

Average branched actin network boundary opposite to the leading edge membrane

In a small time interval $\Delta t = (t - t+\Delta t)$, the number of branches (ΔN) that have dissociated from the small sampled volume ΔV is given by

$$\Delta N = \left([branch]_{t+\Delta t} - [branch]_t\right)\Delta V = \frac{d[branch]_t}{dt}\Delta V \Delta t \tag{S59,}$$

and those dissociated branches during Δt have lifetime $\tau = t$. Therefore, the average lifetime ($\bar{\tau}$) of branches dissociated at different times is given by

$$\bar{\tau} = \frac{\sum_n t_n \Delta N\left(t_n\right)}{\sum_n \Delta N\left(t_n\right)} = \frac{\int_0^\infty t\frac{d[branch]_t}{dt}\Delta V dt}{\int_0^\infty \frac{d[branch]_t}{dt}\Delta V dt}$$

$$= \frac{t[branch]\big|_0^\infty - \int_0^\infty [branch]_t\, dt}{[branch]\big|_{t=\infty} - [branch]\big|_{t=0}} = \frac{\int_0^\infty [branch]_t\, dt}{[branch_1]_0} \qquad \text{S60}$$

According to the time-dependent branch concentration expression in Eqs. S55 or S56, the boundary values, $[branch]|_{t=\infty} = t[branch]|_{t=\infty} = t[branch]|_{t=\infty} = 0$ and $[branch]|_{t=0} = [branch_1]_0$ can be evaluated easily. When $k_{2,F} \neq k_{1.F} + k_{conv,F}$, according to Eq. S55, the average lifetime ($\bar{\tau}$) in Eq. S60 becomes

$$= \int_0^\infty \frac{\left(k_{2,F} - k_{1,F}\right) e^{-\left(k_{1,F}+k_{conv,F}\right)t} - k_{conv,F} e^{-k_{2,F}t}}{k_{2,F} - k_{1,F} - k_{conv,F}}\, dt$$

$$= \left. \frac{-\frac{k_{2,F} - k_{1,F}}{k_{1,F} + k_{conv,F}} e^{-\left(k_{1,F}+k_{conv,F}\right)t} + \frac{k_{conv,F}}{k_{2,F}} e^{-k_{2,F}t}}{k_{2,F} - k_{1,F} - k_{conv,F}} \right|_0^\infty$$

$$= \frac{\frac{k_{2,F} - k_{1,F}}{k_{1,F} + k_{conv,F}} - \frac{k_{conv,F}}{k_{2,F}}}{k_{2,F} - k_{1,F} - k_{conv,F}}, \quad k_{2,F} \neq k_{1,F} + k_{conv,F} \qquad \text{S61.}$$

When $k_{2,F} = k_{1.F} + k_{conv,F}$, according to Eq. S56, the average lifetime ($\bar{\tau}$) becomes

$$= \int_0^\infty \left(1 + k_{conv,F} t\right) e^{-k_{2,F}t} dt = -\frac{1}{k_{2,F}} \left(\left(1 + k_{conv,F} t\right) e^{-k_{2,F}t} \Big|_0^\infty - \int_0^\infty k_{conv,F} e^{-k_{2,F}t} dt \right)$$

$$= \frac{1}{k_{2,F}} \left(1 + \frac{k_{conv,F}}{k_{2,F}} \right), \quad k_{2,F} = k_{1,F} + k_{conv,F} \qquad \text{S62.}$$

All branches in an actin network dissociate at average time as expressed in Eq. S61 or S62. At the average lifetime ($\bar{\tau}$), the average length of the branch distribution ($\bar{d}$; i.e. the distance, or "decay length" at which all branches dissociate) away from membrane in the *x*-direction is given by:

$$\bar{d} = v\bar{t} = \begin{cases} v \dfrac{\frac{k_{2,F} - k_{1,F}}{k_{1,F} + k_{conv,F}} - \frac{k_{conv,F}}{k_{2,F}}}{k_{2,F} - k_{1,F} - k_{conv,F}}, & k_{2,F} \neq k_{1,F} + k_{conv,F} \\ v \dfrac{1}{k_{2,F}} \left(1 + \dfrac{k_{conv,F}}{k_{2,F}} \right), & k_{2,F} = k_{1,F} + k_{conv,F} \end{cases} \qquad \text{S63.}$$

For branches whose time after formation is shorter than the average branch lifetime, their distance away from membrane is shorter than the "decay length" and the population does not dissociate completely. Therefore, this

average distance in *x*-direction ($\bar{d}$; Eq. S63) is also the average length, of the branched actin network from the cell membrane at the cell leading edge in the *x*-direction.

Effects of force on the branched actin network architecture

The results presented in this study indicate that in the absence of force (F = 0), $k_{2,F} = k_{1.F} \sim 0.01$ min^{-1}. Eq. S57 predicts that the branched actin network distribution along *x*-axis follows a single exponential according to:

$$[branch] = [branch_1]_{0,F=0} e^{-\frac{k_{2,F}x}{\nu}} = [branch_1]_{0,F=0} e^{-0.01\frac{x}{\nu}} \quad \text{S64}$$

and according to Eq. S63, the network length in the *x*-direction is given by:

$$\bar{d} = \nu \frac{\frac{k_{2,F} - k_{1,F}}{k_{1,F} + k_{conv,F}} - \frac{k_{conv,F}}{k_{2,F}}}{k_{2,F} - k_{1,F} - k_{conv,F}} = \frac{\nu}{k_{2,F}} = 100\nu \quad \text{S65.}$$

Under 500 μL min^{-1} flow rate, the average force F is ~1 pN for 1.5 μm branch length, and $k_{1.F}+k_{conv,F} \sim 0.32$ and $k_{2,F} \sim 6.67$ min^{-1} (Eq. S41). Under these conditions, the branch distribution (Eq. S57) is given by:

$$\begin{aligned}
[branch] &= \frac{[branch_1]_{0,F}}{k_{2,F} - k_{1,F} - k_{conv,F}} \left(\left(k_{2,F} - k_{1,F}\right) e^{-\frac{\left(k_{1,F} + k_{conv,F}\right)x}{\nu}} - k_{conv,F} e^{-\frac{k_{2,F}x}{\nu}} \right) \\
&= \frac{[branch_1]_{0,F}}{6.67 - 0.32} \left(\left(6.67 - k_{1,F}\right) e^{-\frac{0.32x}{\nu}} - k_{conv,F} e^{-\frac{6.67x}{\nu}} \right) \\
&\sim \frac{[branch_1]_{0,F}}{6.67} \left(6.67 e^{-\frac{0.32x}{\nu}} - k_{conv,F} e^{-\frac{6.67x}{\nu}} \right) \\
&= [branch_1]_{0,F} e^{-\frac{6.67x}{\nu}} \left(e^{\frac{6.67-0.32}{\nu}x} - \frac{k_{conv,F}}{6.67} \right) \\
&\sim [branch_1]_{0,F} \left(e^{-\frac{0.32x}{\nu}} - 0 \right) = [branch_1]_{0,F} e^{-\frac{0.32x}{\nu}}
\end{aligned} \quad \text{S66.}$$

Since $k_{1.F}+k_{conv,F} \sim 0.32$ min^{-1}, the maximum value of $k_{1.F}$ and $k_{conv,F}$ is 0.32 << $k_{2,F} \sim 6.67$ min^{-1}. Also, $e^{\frac{6.67-0.32}{\nu}x} = e^{\frac{6.35}{\nu}x} > 1 >> \frac{k_{conv}}{6.67}$. Under those approximations, the branch density distribution is approximately a single exponential as well and its average length in *x*-direction is given by:

$$\bar{d} = \nu \frac{\frac{k_{2,F} - k_{1,F}}{k_{1,F} + k_{conv,F}} - \frac{k_{conv,F}}{k_{2,F}}}{k_{2,F} - k_{1,F} - k_{conv,F}} \sim \nu \frac{\frac{6.67 - 0}{0.32} - 0}{6.67 - 0.32} \sim \frac{\nu}{0.32} \sim 3\nu \quad \text{S67}$$

Comparison of the branch distribution and average network length with and without pico-newton force (Eqs. S64 vs. S66 and S65 vs. S67), indicates that the branch distribution decay 32 times faster and average length of the branched network in the *x*-direction is 32-fold shorter, or narrower under force.

This comparison is one example how force would modify branched actin network architecture, and assumes similar network velocity v with and without force. The value of v can change with force, and the branched actin network density decay rate constant and network length would change according to Eqs. S57 or S58, and S63. In addition, force could potentially affect the branch formation at the membrane, which would also cause the initial branch concentration $[branch_1]_0$ at the membrane region to change. Note, however, that changes in Arp2/3 complex activation affect only the amplitude of the network density decay, not the decay constant or average network length along the *x*-direction. The effect of force on preferentially debranching of "old" ADP-Arp 2/3 complex branches over young ADP-P_i Arp2/3 complexes shortens the decay length (e.g. narrows the network).

Eqs. S66 and S67 hold under any force, provided that "old" branches with ADP Arp2/3 complex dissociate much faster (given by $k_{2,F}$) than "young" branches with ADP-P_i-Arp2/3 complex (given by $k_{1,F}$) combined with conversion (given by $k_{conv,F}$; i.e. $k_{2,F} >> k_{1,F} + k_{conv,F}$). When these conditions are satisfied, the branched actin network distribution follows a single exponential with a decay constant proportional to $k_{1.F}+k_{conv,F}$ (Eq. S66) and the network average length is inversely proportional to $k_{1.F}+k_{conv,F}$ (Eq. S67).

We now consider only cases in which this condition applies. Assuming the debranching and conversion rate constants are force sensitive and related through Bell's equation (Eq. 1 in main text), substituting Bell's equation to Eqs. S66 and S67 yields the force dependence of branched network distribution and average network length:

$$[branch] \sim [branch_1]_{0,F} e^{-\frac{\left(k_{1,F}+k_{conv}\right)x}{v}} = [branch_1]_{0,F} e^{-\frac{\left(k_{1,F=0}e^{-Fd_1/k_BT}+k_{conv,F=0}e^{-Fd_{conv}/k_BT}\right)x}{v}} \quad \text{S68}$$

$$\bar{d} \sim \frac{v}{k_{1,F}+k_{conv}} = \frac{v}{k_{1,F=0}e^{-Fd_1/k_BT}+k_{conv,F=0}e^{-Fd_{conv}/k_BT}} \quad \text{S69.}$$

The average branch density across the actin filament network for a network distribution following a single exponential decay can be calculated by the following integration.

$$\overline{[branch]}_F = \frac{\int_0^\infty \left([branch]\right)^2 dx}{\int_0^\infty [branch]dx} = \frac{\int_0^\infty \left([branch_1]_{0,F} e^{-\frac{\left(k_{1,F}+k_{conv,F}\right)x}{v}} \right)^2 dx}{\int_0^\infty [branch_1]_{0,F} e^{-\frac{\left(k_{1,F}+k_{conv,F}\right)x}{v}} dx} \quad \text{S70,}$$

$$= \frac{[branch_1]_{0,F}}{2} \frac{\Gamma(1)}{\Gamma(1)} = \frac{[branch_1]_{0,F}}{2}$$

where $\Gamma(x) = \int_0^\infty t^{x-1} e^{-t} dt$ is gamma function and Γ(1) = 1. Therefore, the average branch density is half of the initial density of branches formed at membrane (amplitude) and is determined only by the amplitude independent of the network density decay constant.

This minimal model does not consider debranching by other factors and regulatory proteins such as GMF and cofilin. If the contribution of these debranching proteins is accounted for, the branched actin network would decay even faster and the network length would be even narrower. Note that the preferential dissociation of "old" branches by GMF will introduce effects to those of force.

Fig. S10 illustrates actin network branch density distribution along the *x*-direction in the presence or absence of force with different levels of branch formation at the leading edge ($[branch_1]_{0,F}$). When the total number of branches in the network is conserved and Arp2/3 complexes released from branches are rapidly recycled at the leading edge, the new branch formation at the leading edge ($[branch_1]_{0,F}$) increases in proportion to the enhanced debranching under force.

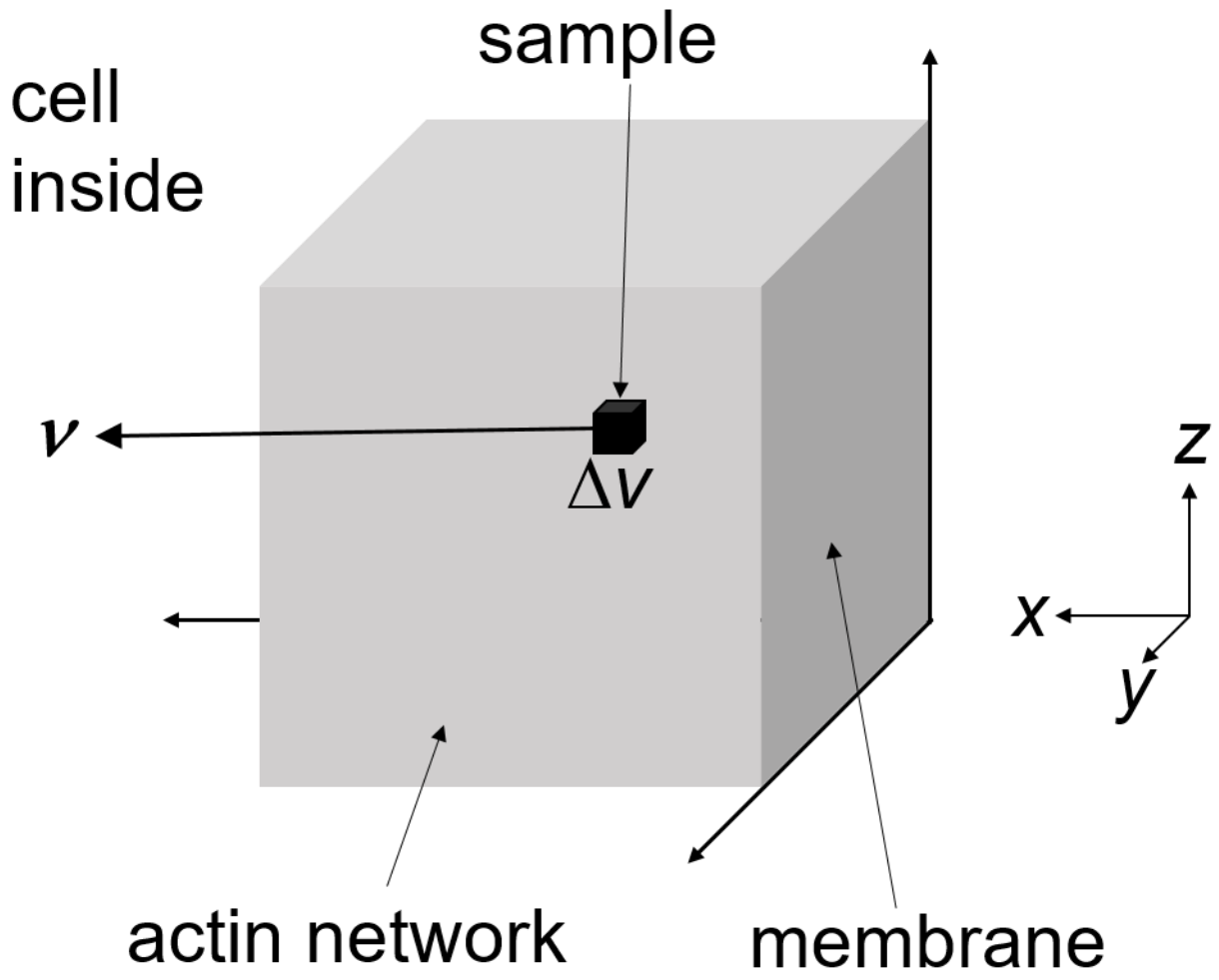

Figure S9: Illustration of the actin branched network formation and internal migration near plasma membrane at the leading edge of a cell. The membrane is on the *y*-*z* plane at $x = 0$. The branched actin network internally migrates by retrograde flow at a constant relative velocity v (x direction) towards the cell interior (grey). We note that the depicted boundaries of the cube do not represent actual network boundaries. The distance between top and bottom edges in *z*-direction is very narrow for lamellipodia and the network is essentially a flat sheet in the *x*-*y* plane.

.

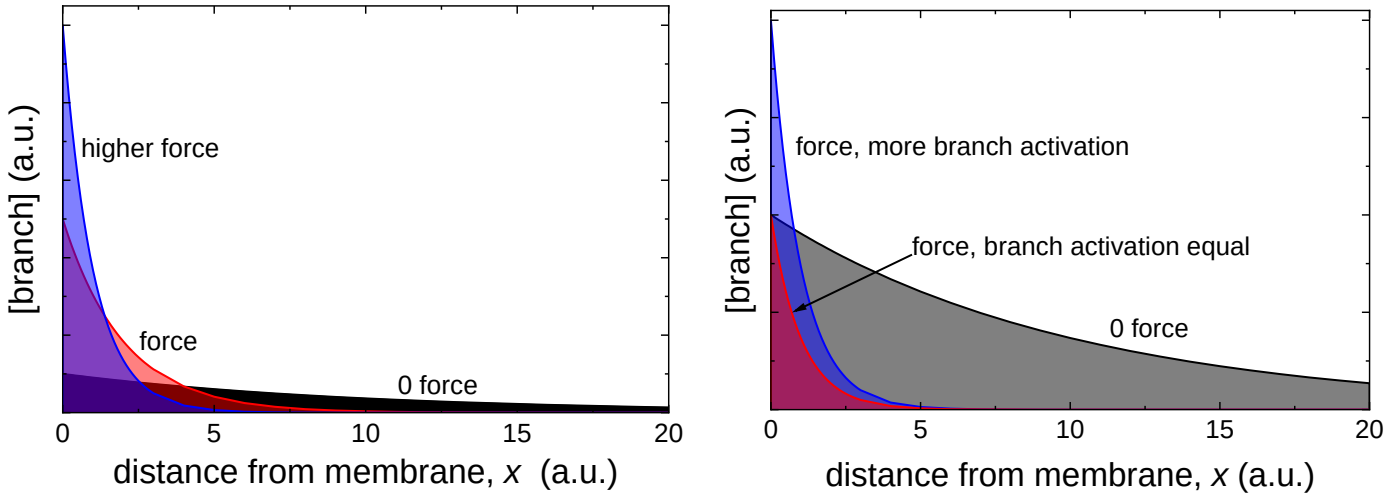

Figure S10. Calculation using Eq. S66 of the distributions of actin filament branches in the leading edge networks in the presence and absence of force. Left: Comparison of the distribution of branches in the network under no force (black), an arbitrary force ("force"; red) and a second arbitrary, but higher force ("higher force"; blue), under conditions when the total number of branches in the network is constant. The decay constants were chosen to be 5-fold larger than in the absence of force for "certain force" and 10-fold higher for the "higher force," both less than the 32-fold change in the decay constant caused by low pN forces in our experiments (Eqs. S64 and S66). Right: Comparison of the distribution of branches in the network with (red and blue) and without (grey) force when branch formation at the leading edge is higher under force (i.e. total number of branches is not necessarily conserved). The decay constant under force was set to be 10-fold larger than in the absence of force. Increasing branch formation 2-fold under force (blue) increases the average network branch density across the network 2-fold (Eq. S70), but decreases, in this special case, the total number of branches in the network (total area under curve) compared to no force (grey). On the other hand, when branch formation at the leading edge is not activated by force (red), the average branch density across the network is the same as in the absence of force (Eq. S70), but the total number of branches decreases.

Part 4. DNA sequence of GMF

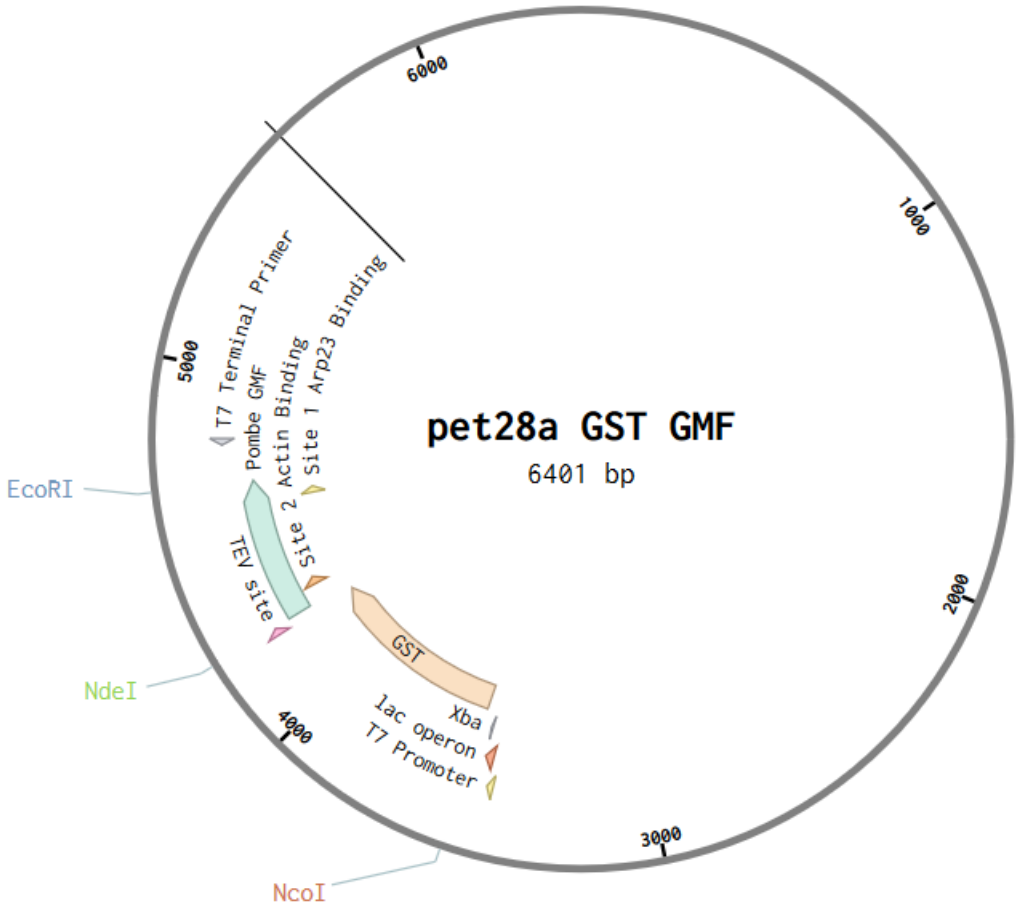

GMF (Glia Maturation Factor) Pombe DNA Sequence:
ATGTCATCAGAGGCTCGTATGTTCACCATTTCGGATACCACGATGAAAGAAATTGATCGATTTCGT
TTGCGGTTGAAGAAATCAGTTATGTATGCTTTCATTCTCAAGGTTGATAAAGCTACTAAGGAGATT
GTTCCCGATGGAGAAATCATGGATTTACAGAGTATTGAAGAGGTCGCAGATGAACTCTCGGAAAC
AAATCCTAGATTTATCCTTGTTTCCTATCCTACCAAAACCACAGATGGTCGACTTAGTACTCCATTG
TTTATGATATACTGGAGACCAAGTGCTACCCCAAATGACTTATCTATGATTTATGCTTCTGCTAAA
GTCTGGTTTCAAGATGTGTCGCAGGTGCACAAAGTATTTGAAGCTAGAGATTCTGAAGATATTACT
AGTGAAGCAGTTGATGAGTTTTTGCATTAA

Pet28A-GST-GMF DNA Sequence
TTGCAAACAAAAAAACCACCGCTACCAGCGGTGGTTTGTTTGCCGGATCAAGAGCTACCAACTCTT
TTTCCGAAGGTAACTGGCTTCAGCAGAGCGCAGATACCAAATACTGTCCTTCTAGTGTAGCCGTAG
TTAGGCCACCACTTCAAGAACTCTGTAGCACCGCCTACATACCTCGCTCTGCTAATCCTGTTACCA
GTGGCTGCTGCCAGTGGCGATAAGTCGTGTCTTACCGGGTTGGACTCAAGACGATAGTTACCGGAT
AAGGCGCAGCGGTCGGGCTGAACGGGGGGTTCGTGCACACAGCCCAGCTTGGAGCGAACGACCT
ACACCGAACTGAGATACCTACAGCGTGAGCTATGAGAAAGCGCCACGCTTCCCGAAGGGAGAAA
GGCGGACAGGTATCCGGTAAGCGGCAGGGTCGGAACAGGAGAGCGCACGAGGGAGCTTCCAGGG

GGAAACGCCTGGTATCTTTATAGTCCTGTCGGGTTTCGCCACCTCTGACTTGAGCGTCGATTTTTGT
GATGCTCGTCAGGGGGGCGGAGCCTATGGAAAAACGCCAGCAACGCGGCCTTTTTACGGTTCCTG
GCCTTTTGCTGGCCTTTTGCTCACATGTTCTTTCCTGCGTTATCCCCTGATTCTGTGGATAACCGTAT
TACCGCCTTTGAGTGAGCTGATACCGCTCGCCGCAGCCGAACGACCGAGCGCAGCGAGTCAGTGA
GCGAGGAAGCGGAAGAGCGCCTGATGCGGTATTTTCTCCTTACGCATCTGTGCGGTATTTCACACC
GCATATATGGTGCACTCTCAGTACAATCTGCTCTGATGCCGCATAGTTAAGCCAGTATACACTCCG
CTATCGCTACGTGACTGGGTCATGGCTGCGCCCCGACACCCGCCAACACCCGCTGACGCGCCCTG
ACGGGCTTGTCTGCTCCCGGCATCCGCTTACAGACAAGCTGTGACCGTCTCCGGGAGCTGCATGTG
TCAGAGGTTTTCACCGTCATCACCGAAACGCGCGAGGCAGCTGCGGTAAAGCTCATCAGCGTGGT
CGTGAAGCGATTCACAGATGTCTGCCTGTTCATCCGCGTCCAGCTCGTTGAGTTTCTCCAGAAGCG
TTAATGTCTGGCTTCTGATAAAGCGGGCCATGTTAAGGGCGGTTTTTTCCTGTTTGGTCACTGATGC
CTCCGTGTAAGGGGGATTTCTGTTCATGGGGGTAATGATACCGATGAAACGAGAGAGGATGCTCA
CGATACGGGTTACTGATGATGAACATGCCCGGTTACTGGAACGTTGTGAGGGTAAACAACTGGCG
GTATGGATGCGGCGGGACCAGAGAAAAATCACTCAGGGTCAATGCCAGCGCTTCGTTAATACAGA
TGTAGGTGTTCCACAGGGTAGCCAGCAGCATCCTGCGATGCAGATCCGGAACATAATGGTGCAGG
GCGCTGACTTCCGCGTTTCCAGACTTTACGAAACACGGAAACCGAAGACCATTCATGTTGTTGCTC
AGGTCGCAGACGTTTTGCAGCAGCAGTCGCTTCACGTTCGCTCGCGTATCGGTGATTCATTCTGCT
AACCAGTAAGGCAACCCCGCCAGCCTAGCCGGGTCCTCAACGACAGGAGCACGATCATGCGCACCC
CGTGGGGCCGCCATGCCGGCGATAATGGCCTGCTTCTCGCCGAAACGTTTGGTGGCGGGACCAGT
GACGAAGGCTTGAGCGAGGGCGTGCAAGATTCCGAATACCGCAAGCGACAGGCCGATCATCGTC
GCGCTCCAGCGAAAGCGGTCCTCGCCGAAAATGACCCAGAGCGCTGCCGGCACCTGTCCTACGAG
TTGCATGATAAAGAAGACAGTCATAAGTGCGGCGACGATAGTCATGCCCCGCGCCCACCGGAAGG
AGCTGACTGGGTTGAAGGCTCTCAAGGGCATCGGTCGAGATCCCGGTGCCTAATGAGTGAGCTAA
CTTACATTAATTGCGTTGCGCTCACTGCCCGCTTTCCAGTCGGGAAACCTGTCGTGCCAGCTGCATT
AATGAATCGGCCAACGCGCGGGGAGAGGCGGTTTGCGTATTGGGCGCCAGGGTGGTTTTTCTTTTC
ACCAGTGAGACGGGCAACAGCTGATTGCCCTTCACCGCCTGGCCCTGAGAGAGTTGCAGCAAGCG
GTCCACGCTGGTTTGCCCCAGCAGGCGAAAATCCTGTTTGATGGTGGTTAACGGCGGGATATAAC
ATGAGCTGTCTTCGGTATCGTCGTATCCCACTACCGAGATATCCGCACCAACGCGCAGCCCGGACT
CGGTAATGGCGCGCATTGCGCCCAGCGCCATCTGATCGTTGGCAACCAGCATCGCAGTGGGAACG
ATGCCCTCATTCAGCATTTGCATGGTTTGTTGAAAACCGGACATGGCACTCCAGTCGCCTTCCCGT
TCCGCTATCGGCTGAATTTGATTGCGAGTGAGATATTTATGCCAGCCAGCCAGACGCAGACGCGCC
GAGACAGAACTTAATGGGCCCGCTAACAGCGCGATTTGCTGGTGACCCAATGCGACCAGATGCTC
CACGCCCAGTCGCGTACCGTCTTCATGGGAGAAAATAATACTGTTGATGGGTGTCTGGTCAGAGA
CATCAAGAAATAACGCCGGAACATTAGTGCAGGCAGCTTCCACAGCAATGGCATCCTGGTCATCC
AGCGGATAGTTAATGATCAGCCCACTGACGCGTTGCGCGAGAAGATTGTGCACCGCCGCTTTACA
GGCTTCGACGCCGCTTCGTTCTACCATCGACACCACCACGCTGGCACCCAGTTGATCGGCGCGAGA
TTTAATCGCCGCGACAATTTGCGACGGCGCGTGCAGGGCCAGACTGGAGGTGGCAACGCCAATCA
GCAACGACTGTTTGCCCGCCAGTTGTTGTGCCACGCGGTTGGGAATGTAATTCAGCTCCGCCATCG
CCGCTTCCACTTTTTCCCGCGTTTTCGCAGAAACGTGGCTGGCCTGGTTCACCACGCGGGAAACGG
TCTGATAAGAGACACCGGCATACTCTGCGACATCGTATAACGTTACTGGTTTCACATTCACCACCC
TGAATTGACTCTCTTCCGGGCGCTATCATGCCATACCGCGAAAGGTTTTGCGCCATTCGATGGTGT
CCGGGATCTCGACGCTCTCCCTTATGCGACTCCTGCATTAGGAAGCAGCCCAGTAGTAGGTTGAGG
CCGTTGAGCACCGCCGCCGCAAGGAATGGTGCATGCAAGGAGATGGCGCCCAACAGTCCCCCGGC
CACGGGGCCTGCCACCATACCCACGCCGAAACAAGCGCTCATGAGCCCGAAGTGGCGAGCCCGAT
CTTCCCCATCGGTGATGTCGGCGATATAGGCGCCAGCAACCGCACCTGTGGCGCCGGTGATGCCG
GCCACGATGCGTCCGGCGTAGAGGATCGAGATCTCGATCCCGCGAAATTAATACGACTCACTATA

GGGGAATTGTGAGCGGATAACAATTCCCCTCTAGAAATAATTTTGTTTAACTTTAAGAAGGAGATA
TACCATGggcCatcatcatcatcatcatTCCCCTATACTAGGTTATTGGAAAATTAAGGGCCTTGTGCAACCCA
CTCGACTTCTTTTGGAATATCTTGAAGAAAAATATGAAGAGCATTTGTATGAGCGCGATGAAGGTG
ATAAATGGCGAAACAAAAAGTTTGAATTGGGTTTGGAGTTTCCCAATCTTCCTTATTATATTGATG
GTGATGTTAAATTAACACAGTCTATGGCCATCATACGTTATATAGCTGACAAGCACAACATGTTGG
GTGGTTGTCCAAAAGAGCGTGCAGAGATTTCAATGCTTGAAGGAGCGGTTTTGGATATTAGATAC
GGTGTTTCGAGAATTGCATATAGTAAAGACTTTGAAACTCTCAAAGTTGATTTTCTTAGCAAGCTA
CCTGAAATGCTGAAAATGTTCGAAGATCGTTTATGTCATAAAACATATTTAAATGGTGATCATGTA
ACCCATCCTGACTTCATGTTGTATGACGCTCTTGATGTTGTTTTATACATGGACCCAATGTGCCTGG
ATGCGTTCCCAAAATTAGTTTGTTTTAAAAAACGTATTGAAGCTATCCCACAAATTGATAAGTACT
TGAAATCCAGCAAGTATATAGCATGGCCTTTGCAGGGCTGGCAAGCCACGTTTGGTGGTGGCGAC
CATCCTCCAAAAGAAAACCTGTATTTTCAGGGCCATATGTCATCAGAGGCTCGTATGTTCACCATT
TCGGATACCACGATGAAAGAAATTGATCGATTTCGTTTGCGGTTGAAGAAATCAGTTATGTATGCT
TTCATTCTCAAGGTTGATAAAGCTACTAAGGAGATTGTTCCCGATGGAGAAATCATGGATTTACAG
AGTATTGAAGAGGTCGCAGATGAACTCTCGGAAACAAATCCTAGATTTATCCTTGTTTCCTATCCT
ACCAAAACCACAGATGGTCGACTTAGTACTCCATTGTTTATGATATACTGGAGACCAAGTGCTACC
CCAAATGACTTATCTATGATTTATGCTTCTGCTAAAGTCTGGTTTCAAGATGTGTCGCAGGTGCAC
AAAGTATTTGAAGCTAGAGATTCTGAAGATATTACTAGTGAAGCAGTTGATGAGTTTTTGCATaagtg
taagTAAGAATTCGAGCTCCGTCGACAAGCTTGCGGCCGCACTCGAGCACCACCACCACCACCACTG
AGATCCGGCTGCTAACAAAGCCCGAAAGGAAGCTGAGTTGGCTGCTGCCACCGCTGAGCAATAAC
TAGCATAACCCCTTGGGGCCTCTAAACGGGTCTTGAGGGGTTTTTTGCTGAAAGGAGGAACTATAT
CCGGATTGGCGAATGGGACGCGCCCTGTAGCGGCGCATTAAGCGCGGCGGGTGTGGTGGTTACGC
GCAGCGTGACCGCTACACTTGCCAGCGCCCTAGCGCCCGCTCCTTTCGCTTTCTTCCCTTCCTTTCT
CGCCACGTTCGCCGGCTTTCCCCGTCAAGCTCTAAATCGGGGGCTCCCTTTAGGGTTCCGATTTAG
TGCTTTACGGCACCTCGACCCCAAAAAACTTGATTAGGGTGATGGTTCACGTAGTGGGCCATCGCC
CTGATAGACGGTTTTTCGCCCTTTGACGTTGGAGTCCACGTTCTTTAATAGTGGACTCTTGTTCCAA
ACTGGAACAACACTCAACCCTATCTCGGTCTATTCTTTTGATTTATAAGGGATTTTGCCGATTTCGG
CCTATTGGTTAAAAAATGAGCTGATTTAACAAAAATTTAACGCGAATTTTAACAAAATATTAACGT
TTACAATTTCAGGTGGCACTTTTCGGGGAAATGTGCGCGGAACCCCTATTTGTTTATTTTTCTAAAT
ACATTCAAATATGTATCCGCTCATGAATTAATTCTTAGAAAAACTCATCGAGCATCAAATGAAACT
GCAATTTATTCATATCAGGATTATCAATACCATATTTTTGAAAAAGCCGTTTCTGTAATGAAGGAG
AAAACTCACCGAGGCAGTTCCATAGGATGGCAAGATCCTGGTATCGGTCTGCGATTCCGACTCGTC
CAACATCAATACAACCTATTAATTTCCCCTCGTCAAAAATAAGGTTATCAAGTGAGAAATCACCAT
GAGTGACGACTGAATCCGGTGAGAATGGCAAAAGTTTATGCATTTCTTTCCAGACTTGTTCAACAG
GCCAGCCATTACGCTCGTCATCAAAATCACTCGCATCAACCAAACCGTTATTCATTCGTGATTGCG
CCTGAGCGAGACGAAATACGCGATCGCTGTTAAAAGGACAATTACAAACAGGAATCGAATGCAA
CCGGCGCAGGAACACTGCCAGCGCATCAACAATATTTTCACCTGAATCAGGATATTCTTCTAATAC
CTGGAATGCTGTTTTCCCGGGGATCGCAGTGGTGAGTAACCATGCATCATCAGGAGTACGGATAA
AATGCTTGATGGTCGGAAGAGGCATAAATTCCGTCAGCCAGTTTAGTCTGACCATCTCATCTGTAA
CATCATTGGCAACGCTACCTTTGCCATGTTTCAGAAACAACTCTGGCGCATCGGGCTTCCCATACA
ATCGATAGATTGTCGCACCTGATTGCCCGACATTATCGCGAGCCCATTTATACCCATATAAATCAG
CATCCATGTTGGAATTTAATCGCGGCCTAGAGCAAGACGTTTCCCGTTGAATATGGCTCATAACAC
CCCTTGTATTACTGTTTATGTAAGCAGACAGTTTTATTGTTCATGACCAAAATCCCTTAACGTGAGT
TTTCGTTCCACTGAGCGTCAGACCCCGTAGAAAAGATCAAAGGATCTTCTTGAGATCCTTTTTTTCT
GCGCGTAATCTGCTGC

References

1. J. A. Cooper, S. B. Walker, T. D. Pollard, Pyrene actin: documentation of the validity of a sensitive assay for actin polymerization. *J Muscle Res Cell Motil* **4**, 253-262 (1983).
2. M. F. Carlier, D. Pantaloni, Binding of Phosphate to F-Adp-Actin and Role of F-Adp-Pi-Actin in Atp-Actin Polymerization. *Journal of Biological Chemistry* **263**, 817-825 (1988).
3. M. F. Carlier, D. Pantaloni, Direct evidence for ADP-Pi-F-actin as the major intermediate in ATP-actin polymerization. Rate of dissociation of Pi from actin filaments. *Biochemistry* **25**, 7789-7792 (1986).
4. M. J. Dayel, R. D. Mullins, Activation of Arp2/3 complex: addition of the first subunit of the new filament by a WASP protein triggers rapid ATP hydrolysis on Arp2. *PLoS Biol* **2**, E91 (2004).
5. C. Le Clainche, D. Pantaloni, M. F. Carlier, ATP hydrolysis on actin-related protein 2/3 complex causes debranching of dendritic actin arrays. *Proc Natl Acad Sci U S A* **100**, 6337-6342 (2003).
6. B. A. Smith, K. Daugherty-Clarke, B. L. Goode, J. Gelles, Pathway of actin filament branch formation by Arp2/3 complex revealed by single-molecule imaging. *Proc Natl Acad Sci U S A* **110**, 1285-1290 (2013).
7. T. D. Pollard, A. G. Weeds, The rate constant for ATP hydrolysis by polymerized actin. *FEBS Lett* **170**, 94-98 (1984).
8. E. Atilgan, D. Wirtz, S. X. Sun, Morphology of the lamellipodium and organization of actin filaments at the leading edge of crawling cells. *Biophys J* **89**, 3589-3602 (2005).
9. M. Vinzenz *et al.*, Actin branching in the initiation and maintenance of lamellipodia. *J Cell Sci* **125**, 2775-2785 (2012).
10. G. L. Ryan, H. M. Petroccia, N. Watanabe, D. Vavylonis, Excitable actin dynamics in lamellipodial protrusion and retraction. *Biophys J* **102**, 1493-1502 (2012).
11. L. M. McMillen, D. Vavylonis, Model of turnover kinetics in the lamellipodium: implications of slow- and fast-diffusing capping protein and Arp2/3 complex. *Phys Biol* **13**, 066009 (2016).
12. T. Miyoshi *et al.*, Actin turnover-dependent fast dissociation of capping protein in the dendritic nucleation actin network: evidence of frequent filament severing. *J Cell Biol* **175**, 947-955 (2006).